The Effect of Time-Scale Truncation and Data Errors on the Linear Relaxation Spectrum.

by
Valérie Gilbert
Chemical Engineering Department
McGill University, Montréal

May 1995

A thesis submitted to the Faculty of Graduate Studies and Research in partial fulfilment of the requirements of the degree of Masters of Engineering

National Library
of Canada

Acquisitions and
Bibliographic Services

395 Wellington Street
Ottawa ON K1A 0N4
Canada

Bibliothèque nationale
du Canada

Acquisitions et
services bibliographiques

395, rue Wellington
Ottawa ON K1A 0N4
Canada

Your file Votre référence

Our file Notre référence

0-612-37298-7

Canada

ABSTRACT

The knowledge of the viscoelastic properties of molten polymers and the ability to predict their behavior under deformation is of prime interest to polymer scientists and industry. The discrete linear relaxation spectrum [G_i, λ_i] is one of the important viscoelastic properties and it is widely used to characterize molten polymers. This spectrum is obtained from experimental values of the dynamic moduli [$G'(\omega)$, $G''(\omega)$]. A linear regression method with and without regularization and a nonlinear regression method were compared for inferring a discrete spectrum from experimental data. Since experimental values are used, errors in the data will affect the reliability of the spectrum. Because of the limitations of the experimental apparatus, the moduli can only be determined over a certain frequency range. The values of the relaxation times (λ_i) and the corresponding elastic moduli (G_i) depend on the range of frequencies over which the storage and loss moduli ($G'(\omega)$ and $G''(\omega)$) are measured and the method used to calculate them. Also, experimental sources of errors such as uncertainty in the gap measurement, variation in the shape of the edge, residual stress due to the preparation of the sample, and temperature uncertainty will induce experimental errors in $G'(\omega)$ and $G''(\omega)$. This work investigates the effect of time-scale truncation and experimental errors on the discrete relaxation spectrum.

RÉSUMÉ

Connaître les propriétés viscoélastiques des polymères a l'état fondu et prédire leur comportement lors de déformations sont parmis les premières préoccupations des scientifiques qui étudient les polymères et de l'industrie. Le spectre de relaxation discret [G_i, λ_i] est une des importantes propriétés viscoélastiques largement utilisées pour caractériser les polymères à l'état fondu. Ce spectre est obtenu a partir des données expérimentales du module dynamique [$G'(\omega)$, $G''(\omega)$]. Une méthode linéaire, avec et sans paramètre de régularisation, et une méthode non linéaire ont été comparées pour déterminer les spectres discrets à partir des données expérimentales. Puisque des valeurs expérimentales sont utilisées, des erreurs affecteront le calcul du spectre. Etant donné les limites de l'appareillage expérimental, le module dynamique n'est déterminé que pour une échelle finie de fréquences. Les valeurs des temps de relaxation (λ_i) et des modules élastiques correspondants (G_i) dépendent de l'échelle de fréquences pour lesquelles les modules d'accumulation et de perte ($G'(\omega)$ et $G''(\omega)$) ont été mesurés et aussi de la méthode utilisée pour déterminer le spectre. De plus, des sources d'erreurs expérimentales telles l'incertitude sur la mesure de l'espacement, la forme du rebord de l'échantillon, le stress résiduel à la préparation des échantillons et l'incertitude sur la température vont induire des erreurs expérimentales sur $G'(\omega)$ et $G''(\omega)$. Cette recherche étudie les effets de la troncature de l'échelle des fréquences de même que les effets des erreurs expérimentales sur le spectre de relaxation discret.

ACKNOWLEDGMENTS

I would like to thank Professor J. M. Dealy for his supervision, Professor Nese Orbey for her comments and explanations regarding her previous research on the subject and Dr M. Fleissner of Hoechst AG for supplying the resin. I would also like to thank my life companion Christian for his presence and assistance and my lab companion Paula for her constant support, our helpful discussions and her help concerning the review of the thesis.

TABLE OF CONTENTS

LIST OF FIGURES

LIST OF TABLES

NOMENCLATURE

A	$2MxN$ matrix containing the dynamic moduli
|AD|	Absolute average deviation between the experimental dynamic moduli and the recalculated dynamic moduli
$G(t, \gamma_0)$	Shear relaxation modulus
$G(t)$	Shear relaxation modulus (linear viscoelasticity)
$[G'(\omega), G''(\omega)]$	Dynamic moduli
$G'(\omega)$	Storage modulus
$G''(\omega)$	Loss modulus
$[G_i, \lambda_i]$	Discrete relaxation spectrum
G_i	Elastic modulus of the i^{th}Maxwell element
$\delta G(\omega_i)$	Correction factor
δG_i	Average correction factor
$G_{avg.}(\omega)$	Average value of G' or G''
$[G'_{corr}, G''_{corr}]$	Corrected dynamic data sets
$[G'_{rec.}, G''_{rec.}]$	Recalculated dynamic moduli
h	Plate spacing or rheometer gap
h_0	Constant to normalized the relaxation modulus G_i
$H(\lambda)$	Continuous relaxation spectrum
$J(t)$	Shear creep compliance
$[J'(\omega), J''(\omega)]$	Dynamic compliance
$J'(\omega)$	Storage compliance
$J''(\omega)$	Loss compliance
M_0	Torque amplitude in oscillatory shear
(Mw)	Weight average molecular weight
(M_w/M_N)	Polydispersity index
N	Number of relaxation times (number of Maxwell parameters (G_i , λ_i))
t	Time
T	Temperature
U	Column orthogonal matrix
$\mathbf{V}^T$	Transpose of an MxM matrix V
W	MxM diagonal matrix containing the singular values
W_{kk}	Singular values

δ	Phase shift (also called mechanical loss angle)
ϕ_0	Angular amplitude for oscillatory shear
$\gamma(t)$	Shear strain
$\dot{\gamma}(t)$	Shear rate (rate of deformation=$d\gamma(t)/dt$)
γ_0	Magnitude of the shear strain
$\delta\gamma(t)$	Small shear strain
$\gamma_{ij}(t')$	Component of infinitesimal strain tensor
η^*	Complex viscosity
λ_i	Relaxation time
$[\lambda_{min.}, \lambda_{max.}]$	Relaxation times range
λ_b	Longest relaxation time
λ_a	Shortest relaxation time
λ^*	Regularization parameter
$\sigma(t)$	Shear stress
σ_0	Stress amplitude
σ	Coefficient of variation of the experimental G' and G'' data
$\sigma^2(G_i)$	Standard error of each element G_i
$\tau_{ij}(t)$	Component of extra stress tensor
ω	Frequency
$(\omega_{min.}, \omega_{max.})$	Frequency range of the dynamic moduli
ω^*	Frequency where the value of $\delta Gi(\omega)$ reaches a plateau

—CHAPTER 1

1. INTRODUCTION

1.1 APPLICATIONS FOR THE RELAXATION SPECTRUM

The relaxation spectrum is used extensively for the modeling of polymer processing (flow modeling) and the analysis of processing experiments. It is also useful for evaluating constitutive equations and simulating transient experiments. The constitutive equation is a mathematical model that describes the relationship between applied stresses and the corresponding deformation responses of polymer melts or vice versa. First, the rheologist has to characterize the flow behavior of a material using a set of tests. Then, using experimental data, he or she wants to predict the behavior of the polymer melt in different flow situations. With the appropriate constitutive equation and relaxation spectra, it is in theory possible to predict the material response for a variety of deformation histories.

The relaxation modulus $G(t)$ is most useful for rheological modeling rather than the dynamic moduli, $G'(\omega)$, $G''(\omega)$, which are easily determined experimentally. The relaxation modulus can be measured directly with the step-stain experiment [30]. Although the analysis is simpler, the accuracy is not as good as for the dynamic mechanical experiment because a step strain deformation can not be generated as precisely as the sinusoidal deformation necessary for the dynamic moduli. It is therefore useful to be able to convert the data from the frequency domain ($G'(\omega)$, $G''(\omega)$) into data in the time domain ($G(t)$) which is easier to interpret. Kamath and Mackley [20] present two methods to determine $G(t)$ from dynamic data using integral functions. Another way to convert from the frequency to the time domain is to use the discrete relaxation spectrum [G_i, λ_i] as an intermediate. As shown by Winter *et al.* [37], nonlinear responses can be calculated if an appropriate model is available, and linear responses can be expressed in an analytic form for specific strain histories.

If the relaxation spectrum is known, other linear viscoelastic material functions can be easily calculated [15]. For example, it is possible to estimate the viscosity value from

the relaxation spectrum. Winter *et al.* [37] present two relations that predict the viscosity from the linear relaxation spectrum: the Cox-Merz relation and the Gleissle mirror relation.

Moreover, the relaxation time spectrum is also useful when we are interested in the relation between the molecular weight or mass distribution and rheological properties. According to Baumgeartel *et al.* [4], correlations between molecular parameters and longest relaxation time can be made.

Finally, if the number of relaxation modes is kept small, the spectrum is convenient for data storage and numerical calculations [2]. It is thus useful for a rheological data bank.

1.2 OBJECTIVES

To know the viscoelastic properties of molten polymers and to be able to predict their behavior under deformation is of great interest to polymer scientists and industry. As presented in the previous section, the discrete linear relaxation spectrum is an important rheological properties and is widely used to characterize molten polymers. This spectrum is inferred from a set of experimental data through a mathematical method as is shown on Figure 1.1.

Since experimental values are used to calculate the discrete spectrum, errors in the data will affect the reliability of the spectrum. Ideally, the range of experimental data should be infinite. In practice, because of the limitations of the experimental apparatus, the moduli can only be determined over a limited frequency range (Figure 1.2). This is especially true at low frequencies where it is difficult and time consuming to obtain values. Time-temperature superposition can often be used to broaden the available frequency window; however with some polymers such as polyethylene this is not possible. The values of the relaxation times (λ_i) and the corresponding relaxation moduli (G_i) depend on the range of frequencies over which the storage and loss moduli are measured and the method used to calculate them.

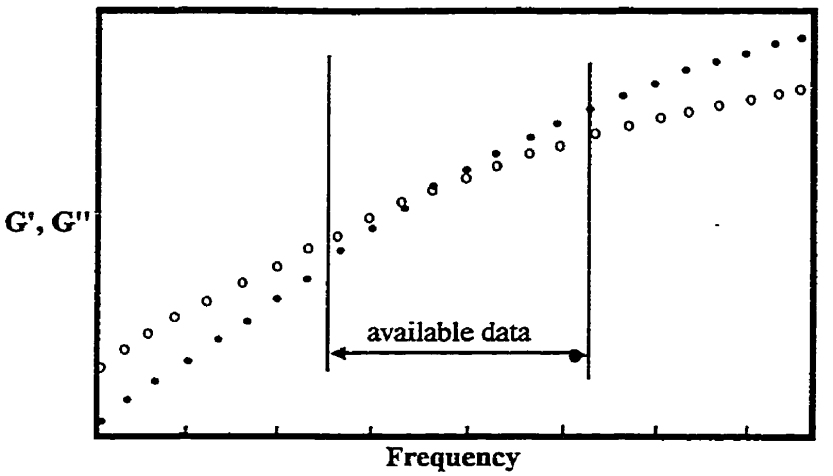

FIGURE 1.2 Experimental window available to infer the discrete spectrum.

The first objective of this research was to compare several methods for inferring a discrete spectrum. From the methods described in the literature we have chosen to study three: linear regression, linear regression with regularization, and nonlinear regression.

The second objective is to study the effects of point density, time-scale truncation of data and experimental errors on the inferred spectra. The impact of these errors was studied for each of the three methods used for three sets of data.

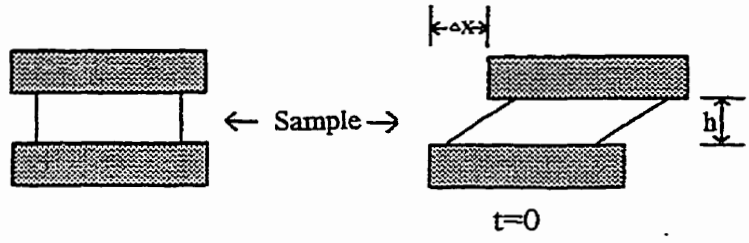

FIGURE 2.1 Stress relaxation experiment.

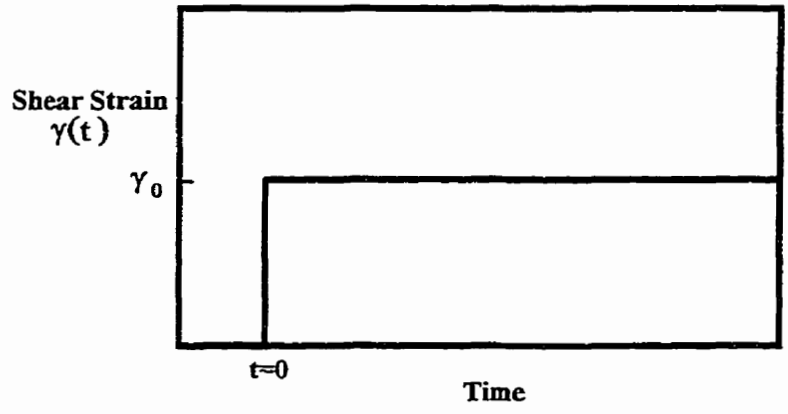

FIGURE 2.2 Shear strain in a stress relaxation experiment.

The resulting stress is measured as a function of time ($\sigma(t)$, Figure 2.3). The shear relaxation modulus, $G(t, \gamma_0)$, is the stress divided by the magnitude of the strain introduced to start the experiment:

$$G(t, \gamma_0) \equiv \sigma(t) / \gamma_0 \qquad 2.2$$

This relaxation modulus is generally a function of the strain magnitude. However, when the strain is very small, as in the case of linear viscoelasticity, the modulus is independent of the strain, and the stress becomes proportional to the strain:

$$\sigma(t) = G(t)\gamma_0 \qquad 2.3$$

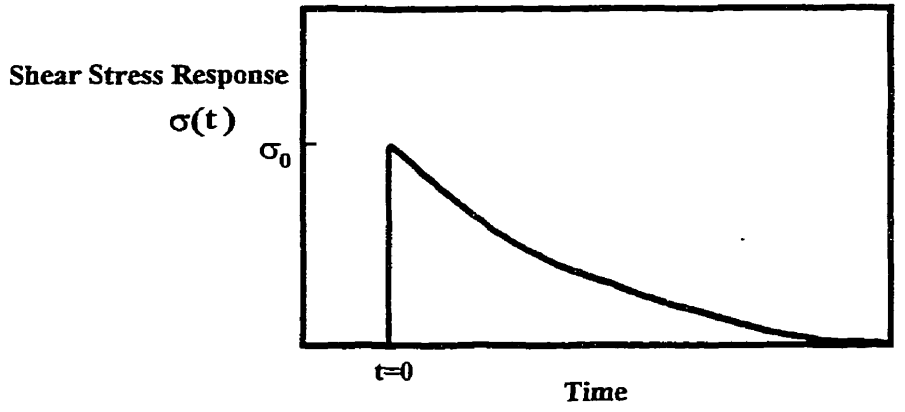

FIGURE 2.3 Shear stress in a stress relaxation experiment.

2.1.2 Boltzmann Superposition Principle

We can derive a general equation, describing all types of linear viscoelastic behavior, starting from the assumption that the relaxation modulus is independent of the strain amplitude. Consider an experiment where the sample is subjected to a sequence of small shear strains: $\delta\gamma(t_1)$, $\delta\gamma(t_2)$, $\delta\gamma(t_3)$...$\delta\gamma(t_N)$ as shown in Figure 2.4.

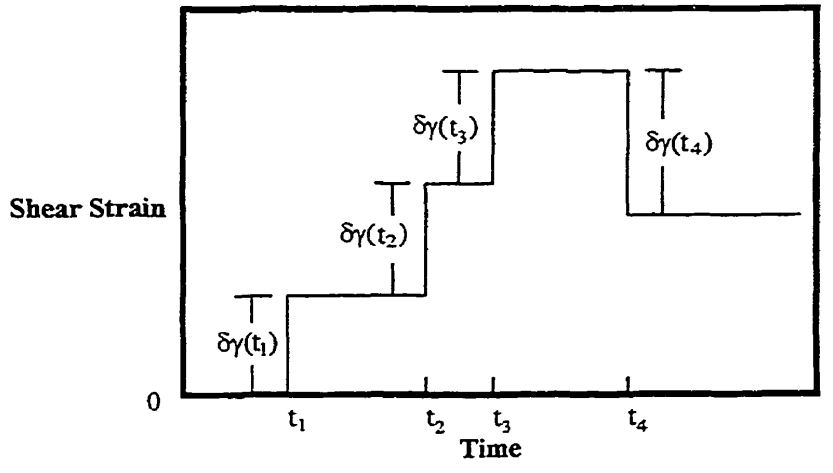

FIGURE 2.4 Sequence of small shear strains.

Because we assume that the response to each step is independent of the previous one, we can simply add or superpose the stresses resulting from the series of strains. For a succession of N small strains, the stress is given by:

$$\sigma(t) = \sum_{i=1}^{N} G(t - t_i)\delta\gamma(t_i) \qquad 2.4$$

If we consider a smooth strain history, instead of the succession of finite steps, we obtain:

$$\sigma(t) = \int_{-\infty}^{t} G(t - t')d\gamma(t') \qquad 2.5$$

Since the rate of deformation γ is equal to $d\gamma(t)/dt$:

$$\sigma(t) = \int_{-\infty}^{t} G(t - t')\dot{\gamma}(t')dt' \qquad 2.6$$

In practice, it is not necessary to know the strain history infinitely far into the past (from $-\infty$ to t) to calculate the stress. We usually start the experiment at some time t=0 when the material is not under stress ($\sigma(0)$=0):

$$\sigma(t) = \int_{0}^{t} G(t - t')d\gamma(t') \qquad 2.7$$

These equations apply only to shearing deformations, but since the relaxation process in linear viscoelasticity is independent not only of the magnitude of the strain but also of the type of deformation (kinematics), the shear stress ($\sigma(t)$) can be replaced by the stress tensor ($\tau_{ij}(t)$) and the shear strain ($\gamma(t')$) can be replaced by the infinitesimal strain tensor ($\gamma_{ij}(t')$). We then obtain the following two alternative forms of the Boltzmann superposition principle:

$$\tau_{ij}(t) = \int_{-\infty}^{t} G(t - t')d\gamma_{ij}(t') \qquad 2.8a$$

$$\tau_{ij}(t) = \int_{-\infty}^{t} G(t - t')\dot{\gamma}_{ij}(t')dt' \qquad 2.8b$$

It is also possible to perform experiments where the stress is the controlled variable and the strain is the observed response. Such an experiment is called a creep test. The results are presented in terms of a material function called the shear creep compliance ($J(t)$) which is defined as the strain divided by the magnitude of the stress introduced to start the experiment. Equation 2.2 is then replaced by Equation 2.9:

$$J(t) \equiv \gamma(t) / \sigma_0 \tag{2.9}$$

The resulting strain is measured as a function of time ($\gamma(t)$). In the case of linear behavior, the creep compliance is independent of σ_0 and the strain becomes proportional to the strain:

$$\gamma(t) = J(t)\sigma_0 \tag{2.10}$$

Starting with Equation 2.10 and using the same development as above, the equivalent of Equation 2.8b for a creep test is:

$$\gamma_{ij}(t) = \int_{-\infty}^{t} J(t-t')\tau_{ij}(t')dt' \tag{2.11}$$

2.1.3 Maxwell Model and Relaxation Spectrum

In principle, if the relaxation modulus ($G(t)$) is determined by any experiment, the linear response to any deformation (Equations 2.8a and 2.8b) can be predicted. It is thus convenient to have an explicit equation for $G(t)$, with parameters that can be evaluated using experimental data.

The most popular approach to use a functional form for the relaxation modulus that is based on the generalized Maxwell model (the details of this model are described in Reference [8]):

$$\tau_{ij}(t) = \int_{-\infty}^{t} \sum G_k \exp[-(t-t') / \lambda_k]\gamma_{ij}(t')dt' \tag{2.12}$$

2.1.4 Small Amplitude Oscillatory Shear

Small amplitude oscillatory shear is the experiment most often used to determine the relaxation spectrum and other linear viscoelastic properties of polymers. During this experiment, a sinusoidal shearing deformation of strain amplitude γ_0 and frequency ω is applied to a sample of melted polymer through the lower plate of the rheometer (Figure 2.5).

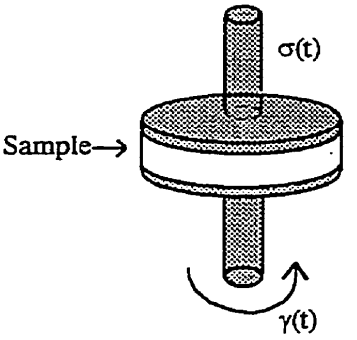

FIGURE 2.5 Parallel disk rheometer.

The shear strain as a function of time is given by:

$$\gamma(t) = \gamma_0 \sin(\omega t) \tag{2.15}$$

By differentiating Equation 2.15, we obtain the shear rate as a function of time:

$$\gamma(t) = \gamma_0 \omega \cos(\omega t) = \gamma_0 \cos(\omega t) \tag{2.16}$$

The shear rate is out of phase by 90° with the shear strain as shown on Figure 2.6.

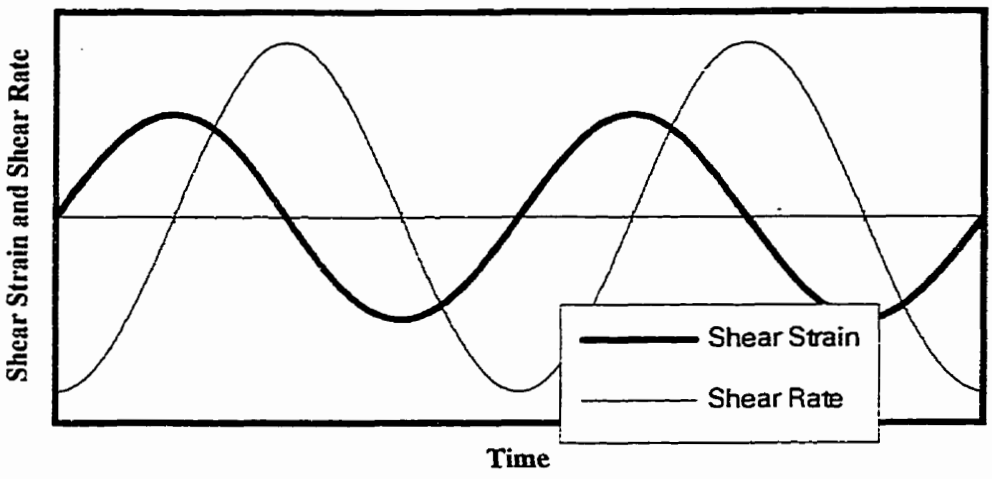

FIGURE 2.6 Comparison of the phase of shear strain and shear rate.

The stress exerted by the sample on the upper plate is measured as a function of time. If the strain amplitude (γ_0) is small, the Boltzmann superposition principle can be used to calculate the stress. By substituting Equation 2.16 into Equation 2.6, we obtain a stress response that is sinusoidal in time and has the same frequency as the strain:

$$\sigma(t) = \sigma_0 \sin(\omega t + \delta) \qquad 2.17$$

where σ_0 is the stress amplitude and δ is a phase shift, also called the mechanical loss angle.

Using a trigonometric identity, we can rewrite Equation 2.17 in a more useful form:

$$\sigma(t) = \gamma_0\left[G'(\omega)\sin(\omega t) + G''(\omega)\cos(\omega t)\right] \qquad 2.18$$

where G' and G'' are the storage and loss moduli, respectively, and are functions of frequency. These two quantities can be interpreted physically in terms of energy storage (G') and loss (G''). In a material where there is no viscous dissipation (purely elastic material), the loss modulus is zero, and in a material where there is no energy storage (purely viscous liquid) , the storage modulus is zero.

2.2.1 Linear Regression

The Maxwell parameters of the discrete relaxation spectrum are found by fitting Equations 2.19a and 2.19b to G' and G'' data (Equations 2.20a and 2.20b). The parameters $[G_i, \lambda_i]$ are determined by minimizing the average square deviation between the predicted G' and G'' values and the measured G' and G'' data (least-squares fit):

$$\sum_{j=1}^{M}\left[\left(\sum_{i=1}^{N}\frac{1}{G'(\omega_j)}G_i\frac{(\omega_j\lambda_i)^2}{1+(\omega_j\lambda_i)^2}-1\right)^2+\left(\sum_{i=1}^{N}\frac{1}{G''(\omega_j)}G_i\frac{\omega_j\lambda_i}{1+(\omega_j\lambda_i)^2}-1\right)^2\right]=\text{Min} \qquad 2.21$$

The user specifies N values of λ_i equally distributed on a logarithmic time scale, within the range of experimental frequencies. The corresponding modulus G_i is subsequently determined. The discrete relaxation spectrum is plotted on a semi-logarithmic or double logarithmic scale because of the different contributions at short and long relaxation times (the contribution of short relaxation times is larger).

Differentiation of the previous equation with respect to each G_i gives sets of equations called normal equations of the linear least-square problem. This system of equations can be solved by Gauss Jordan elimination [26]. However, in many cases the normal equations are very close to singular and Equation 2.21 can be solved by a singular value decomposition (SVD) method to give numerical results [17].

A $2M$xN matrix A and a $2M$x**1** matrix **b** need to be created to apply the SVD method [25]:

$$A_{ji}=\frac{1}{G'(\omega_j)}\frac{(\omega_j\lambda_i)^2}{1+(\omega_j\lambda_i)^2} \qquad 2.22$$

$$A_{(j+M)i}=\frac{1}{G''(\omega_j)}\frac{\omega_j\lambda_i}{1+(\omega_j\lambda_i)^2},\quad j=1,\ldots,M;\quad i=1,\ldots,N \qquad 2.23$$

$$b_k = 1, \quad k = 1, \ldots, M \tag{2.24}$$

The matrix **A** is given by Equation 2.25:

$$\mathrm{A} = \mathrm{U} \cdot \mathrm{W} \cdot \mathrm{V}^T \tag{2.25}$$

$$\begin{bmatrix} \mathrm{A} \end{bmatrix} = \begin{bmatrix} \mathrm{U} \end{bmatrix} \cdot \begin{bmatrix} w_1 & & & \\ & w_2 & & \\ & & \cdots & \\ & & & w_n \end{bmatrix} \cdot \begin{bmatrix} \mathrm{V}^T \end{bmatrix}$$

where **U** is a column orthogonal matrix, **W** is a MxM diagonal matrix with positive or zero elements called the singular values, and $\mathbf{V}^T$ is the transpose of an MxM matrix V. Programs to apply the SVD method are available in many software library packages.

The elastic modulus is given by:

$$G_i = \sum_{k=1}^{N} \frac{1}{W_{kk}} V_{ik} \left(U_k \cdot b \right) \tag{2.26}$$

where U_k (k=1,...,N) represents the N columns of U, each column a vector of length 2M.

The results of G_i alone are insufficient to characterize the spectrum and the standard error on G_i must also be calculated. The standard errors increase with the number of relaxation times and easily become as large or even greater than G_i [17]. The standard error of each element G_i is:

$$\sigma^2(G_i) = \sigma^2 \sum_{k=1}^{N} \frac{1}{W_{kk}^2} \left(V_{ik} \right)^2 \tag{2.27}$$

where σ is the coefficient of variation of the experimental G' and G'' data.

A listing of the Matlab program for the linear regression method is given in Appendix A.

2.2.2 Linear Regression with Regularization

The previous method is somewhat arbitrary and may not lead to a unique, physically meaningful spectrum. In fact, the values of G_i depend on the choice of λ_i and N, and certain choices can lead to negative G_i values, especially as N increases. Negative G_i must be avoided since they are physically unrealistic. Equation 2.27 shows that if some singular values W_{kk} get too small, the errors become large, because the minimum is surrounded by a very flat valley. Also, according to Equation 2.26, small changes in the experimental data may produce huge variations in G_i if some W_{kk} become too small. Consequently, a broad range of possible solutions (with large deviations from each other) is found to fit the data within experimental error. Such a problem as the one encountered with the linear regression method is called ill-posed. Honerkamp *et al.* [16, 17] illustrate the unavoidable problems associated with the linear regression method.

If we are only interested in a representation of one material function, any one of the solutions may be chosen. However, if one is interested in the relaxation spectrum as a physical reality, one would try to pick out the true solution from the whole set of solutions by introducing some further information. There are several methods for solving ill-posed problems, as we will see in the last section, which can be used to find the true solution from the set of possible solutions. The most commonly used is the regularization method of Tikhonov. In order to apply that method, Honerkamp and Weese [17, 18] introduced an additional criterion in Equation 2.21:

$$\sum_{j=1}^{M}\left[\left(\sum_{i=1}^{N}\frac{1}{G'(\omega_j)}G_i\frac{(\omega_j\lambda_i)^2}{1+(\omega_j\lambda_i)^2}-1\right)^2+\left(\sum_{i=1}^{N}\frac{1}{G''(\omega_j)}G_i\frac{\omega_j\lambda_i}{1+(\omega_j\lambda_i)^2}-1\right)^2\right]+\lambda^*\sum_{i=1}^{N}G_i^2=\text{Min} \qquad 2.28$$

where λ^* is the regularization parameter.

Several methods also exist to determine λ^*. If the regularization parameter is too large, the solution will be over smoothed, and if the regularization parameter is too small, the solution is still affected by too large errors. Following several authors [17, 22, 25], we

The nonlinear technique proposed by Baumgeartel and Winter simultaneously adjusts the parameters G_i, λ_i and N of the discrete spectrum to obtain the best fit of G', G''. By keeping not only G_i but also N and λ_i freely adjustable, all the G_i are found to be positive. The method was found to be insensitive to the choice of the initial values ($G_{i,0}$, $\lambda_{i,0}$, N_0).

The number N is adjusted during the iterative calculations depending on the need to avoid ill-posedness and for improved fit. Baumgeartel and Winter found that the problem ill-posedness can be avoided by using a small number of relaxation times. They found that an optimum range of relaxation times that depends upon the material under investigation exists but is not known *a priori*. The choice of N is thus crucial for the success of their method. With too few relaxation modes, the average deviation between data and fit is large. As N increases, the average deviation decreases rapidly. With only a few relaxation times per decade, the fit improves markedly and represents the data within experimental error. Above a certain value of N, the fit does not improve any further. A further increase in the number of relaxation modes is not justified, and the problem becomes ill-posed. At a high value of N, negative G_i values start to occur. Also, in most practical cases the finite number of data points is not sufficient to determine the large number of G_i and λ_i associated with high values of N.

The initial number of relaxation times is chosen between 1 and 2 per decade. The authors found it to be advantageous to start with a large N and let the program eliminate unnecessary relaxation times. The appearance of negative G_i values is one criterion for reducing the number of relaxation modes.

2.2.4 Other Methods

This section briefly presents a few other methods also found in the literature, although these methods were not used in the present work. The list found here is not an exhaustive one, but most of the recent methods are named and briefly introduced.

The methods to calculate the relaxation spectra presented in Section 2.2 are recent. They approach the ill-posed problem in a physical manner with simple and robust numerical methods. These methods incorporate a constraint, a physical criterion, that translates *a priori* knowledge about the solution instead of a strictly numerical criterion.

This permits the avoidance of the problem of ill-posedness and selects the correct solution from a set of otherwise equivalent solutions.

Soskey and Winter [30] used another linear method. They minimized the error between the experimental values G', G'' and then back-calculated dynamic moduli using the method of Marquardt-Levenberg. The appearance of negative frequencies permits one to determine the number of frequencies.

Provencher [27, 28] used a general constrained linear regularization method to circumvent the ill-posed character of the linear problem. The simplest solution that is consistent with prior knowledge and the experimental data is thus found. The method is also available through software named CONTIN. This general method can be applied to the determination of the discrete relaxation spectrum [23]. The problem is formulated as a least squares equation with an added quadratic form, the regularizor, which imposes prior knowledge. Physical constraints (all $G_i \geq 0$) and/or consistency with other independent rheological measurements, can be incorporated into the numerical algorithm. Numerically stable orthogonal decomposition and quadratic programming algorithms are used to obtain the unique global solution. The regularization parameter can be automatically chosen on the basis of an F-test and confidence region.

As was said in Section 2.2.2, several methods exist to determine the regularization parameter of Equation 2.28. In that section, one method, the minimization of the predictive mean-square signal error, was presented. Honerkamp and Weese [18] consider two other methods: the well-known discrepancy principle and the recently developed self-consistency method. These methods are well presented in reference 18. Their conclusion was that the self-consistency method is the most reliable.

Apart from the regularization method, there are other ways to solve ill-posed problems. The maximum entropy method can be found in the literature [10] as well as inferred spectra [11, 16]. A recursive computer algorithm is presented by Emri and Tschoegl [12, 13, 14]. Also, the Padé-Laplace method can be extended to the extraction of the Maxwellian modes from the G' and G'' data [29].

The solutions obtained depend on the errors assumed for the experimental data. Instead of assuming a constant absolute error, Elster and Honerkamp [9] present an error

model. They introduced this *a priori* knowledge or constraint in the regularization method and the maximum entropy method, avoiding the problem of ill-posedness.

Methods to infer the continuous relaxation spectrum are also presented in the literature. The 'Parsimonious Modeling' (program IRIS) developed by Baumgeartel and Winter [2] also determines the continuous spectrum. Weese used the Tikhonov regularization technique to determine the continuous spectrum in his program FTIKREG (Fast TIKhonov REGularization method) [33]. The regularization parameter was determined using the self-consistent method cited previously. Elster *et al.* [11] present some spectra inferred using FTIKREG. Weese also created the program NLREG (NonLinear REGularization) [34, 19]. This nonlinear regularization method is a generalization of the linear regularization method used in the program FTIKREG. Tschoegl [32] presents several methods to derive the continuous spectrum from a step response or a harmonic response. The Regularization-Quadratic Programming (RQP) method also permits the determination of the continuous spectrum and was proposed by Wiff [35, 36]. Finally, a minimax method is presented by Basistov *et al.* [1].

2.3 PREVIOUS WORK

2.3.1 Determination of the Discrete Relaxation Spectrum

Orbey and Dealy [25] compared linear regression with and without a regularization parameter and nonlinear regression. They found that all three methods give similar results for G_i for a given λ_i. In the linear regression without regularization and the nonlinear regression (IRIS), the relaxation times' range chosen [$\lambda_{min.}$, $\lambda_{max.}$] affect the final values of G_i. Furthermore, if, in the case of linear regression, N is small, negative G_i are avoided. In the regularized solution, the chosen range of relaxation times [$\lambda_{min.}$, $\lambda_{max.}$] and the coefficient of variation of the experimental data influence greatly the regularization parameter λ^* and thus the relaxation spectrum. Finally, they concluded that linear regression with regularization gives the best agreement between the experimental dynamic moduli (G' and G'' experimental) and the recalculated moduli based on the discrete spectrum (G' and G'' back-calculated using G_i and λ_i determined by the regularization method).

Baumgaertel and Winter [2] concluded that their method, nonlinear regression, has the advantage of being simply executed by a fully automated program. The solution is also independent of the starting parameters (G_i, λ_i and N). They reported the ability to convert successfully all the data measured in their lab or given to them. They also found [5] that the spectrum is insensitive to data noise or variations in data intensity, which is an unusual situation for a problem recognized as ill-posed. They conclude that increasing the number of λ_i values causes ill-posedness, and this problem is avoided by using a small number of relaxation times.

Elster and Honerkamp [9] in their study of the role of the error model found that the determination of relaxation spectrum using a regularization method gives a spectrum that depends on the error model proposed for the experimental data. In our case, the error model assumed (σ_i=σ=constant) is the most common and simplest one.

Honerkamp and Weese [17] presented the ill-posedness nature of the linear regression method and concluded that the results obtained with that method are entirely unsatisfactory. They then used linear regression with regularization with simulated experimental and real data. They obtained good agreement with the known relaxation spectrum for the simulated data and plausible results for the real data.

Finally, Honerkamp and Weese [18] tested three methods for determining the regularization parameter in the Tikhonov regularization method. For the predictive mean-square signal error method, they obtained reasonably good results, although the best ones were obtained with the self-consistent method that they developed.

2.3.2 Time-Scale Truncation and Data Errors

There has been no exhaustive study of the effect of time-scale truncation. Nothing was found about data errors, from the point of view of interest to us, and nothing was found about point density. The next part will present the conclusions of the few authors who have studied the impact of time-scale truncation on the discrete relaxation spectrum.

Mead [23] looked at the impact of truncation in order to test his numerical interconversion method, with and without integral moment constraint. He considered numerically simulated data [G_i, λ_i] (true solution). First, the data set [G', G''] was twice

truncated at low frequency. The relaxation spectrum was then calculated using the full data set and the two truncated dynamic data sets. Comparing the spectra with the "true" solution, he found that large relaxation times (low frequencies) were more affected. Although the dynamic data were incomplete in the low frequency range, the application of the moment constraints was found to lead the spectra closer to the true solution at large relaxation times.

Honerkamp [16] also considered dynamic data generated from a model spectrum $[G_i, \lambda_i]$. Data were available in the frequency range $10^{-5} \leq \omega \leq 10^{7}$. Two methods were used to determine the spectrum: the regularization method and the maximum entropy method. The data set was then truncated and only values for $\omega \leq 10$ were considered. The inferred spectrum could not be trusted for $\lambda_i \leq 10^{-1}$, but it was still correct for $\lambda_i \geq 10^{-1}$ in the case of the two methods. Information concerning the asymptotic behavior of the dynamic moduli was then included in the two previous methods. This information led the inferred spectrum closer to the "true" solution at lower relaxation times ($\lambda_i \leq 10^{-1}$). Honerkamp concluded that many data points could be left out without seriously deforming the spectrum.

Elster, Honerkamp and Weese [11] found that time-scale truncation can improve the results of the calculation of a continuous relaxation spectrum using the Tikhonov regularization method (program called FTIKREG). They found that difficulties arise if the dynamic moduli are available in the transition region. These difficulties are caused by the considerably different contributions in the spectrum of short and long relaxation times: short relaxation times have a large contribution and describe the rheological properties in the transition and glassy region, and long relaxation times have a small contribution and characterize the rheological properties in the terminal and plateau region. They avoided these difficulties by using the dynamic moduli data only in the terminal and plateau region in the calculation of the relaxation spectrum. Honerkamp and Weese [19] showed, using simulated data, that these difficulties can also be avoided by using a nonlinear regularization method (program called NLREG).

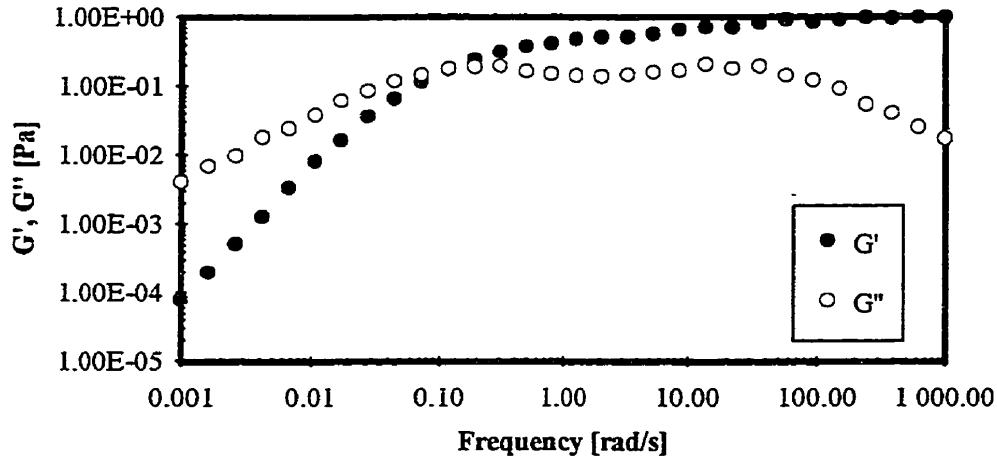

FIGURE 3.2 Dynamic moduli versus frequency (hypothetical material).

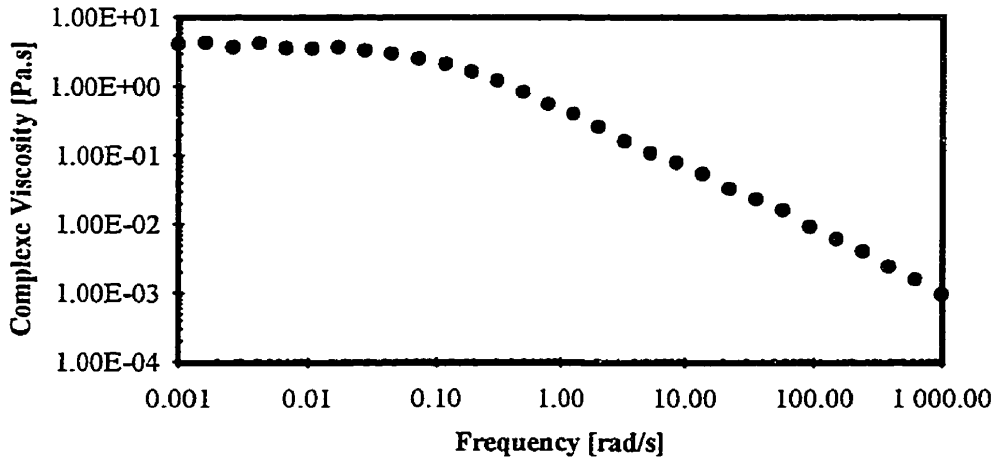

FIGURE 3.3 Complex viscosity versus frequency (hypothetical material).

3.2 HDPE

The second spectrum used was for a high density polyethylene (M_w=3.19x10^{+5} and M_w/M_N=31). The molecular weight distribution information was obtained from gel permeation chromatograghy measurements performed by Hoescht AG, the resin supplier. The dynamic moduli were determined experimentally using a Rheometrics Dynamic Analyser II (RDA II). The experimental and data analysis methods will be described in Chapter 4 and the results will be presented in Chapter 5.

3.3 POLYBUTADIENE

The last data set is for a narrow molecular weight distribution polybutadiene. The experimental data were presented by Honerkamp and Weese [17]. Figure 3.4 and Table B.2 in Appendix B give the experimental storage and loss moduli of the polybutadiene, and Figure 3.5 gives its complex viscosity (Equation 3.1). The coefficient of variation was given as 0.04. This data set was used in order to apply time-scale truncation to a second polymer and to compare the reproducibility of the results.

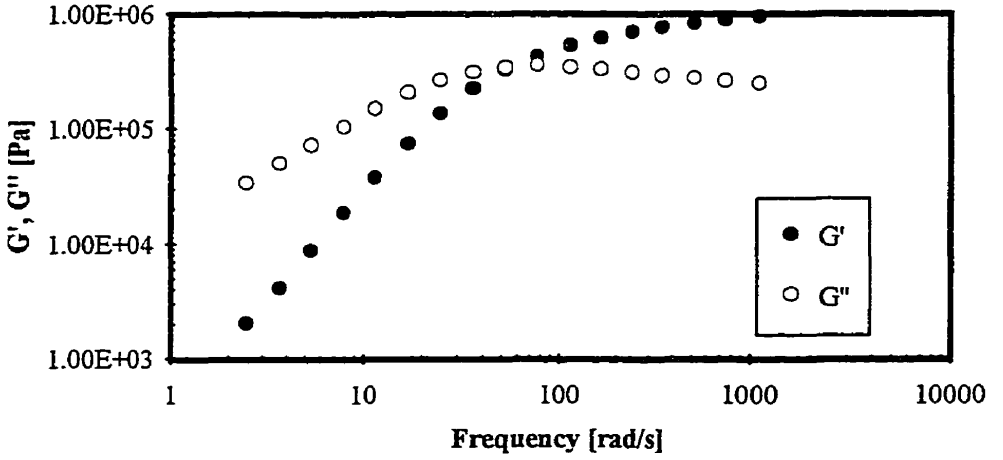

FIGURE 3.4 Dynamic moduli versus frequency for the polybutadiene.

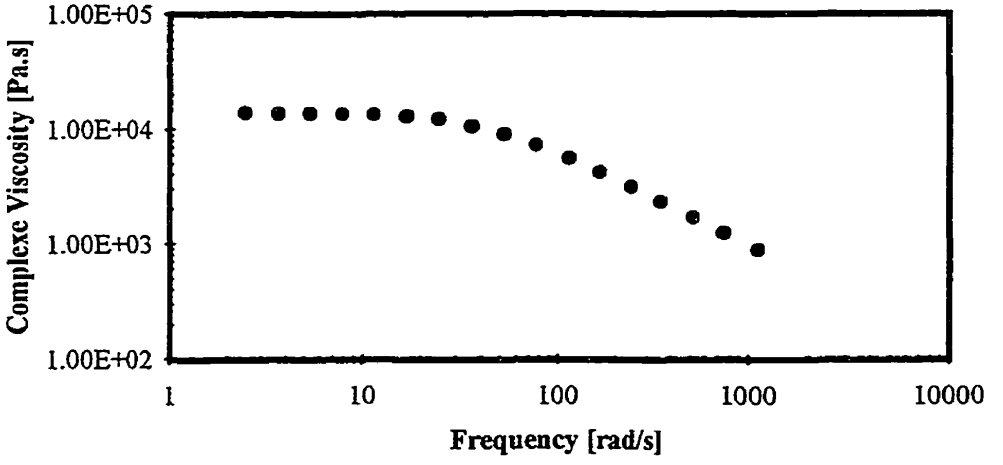

FIGURE 3.5 Complex viscosity versus frequency for the polybutadiene.

—CHAPTER 4—

4. EXPERIMENTAL AND DATA ANALYSIS METHODS

4.1 STRATEGY OF EXPERIMENTATION

4.1.1 Apparatus

The rheometer used was a Rheometrics Dynamic Analyser II (RDA). The experiments were performed at 190°C. The reliable range of the torque transducer is between 5 and 2000 g.cm for this instrument.

4.1.2 Sample Preparation

All the samples were molded using a hydraulic press at 190°C. Two procedures were employed, a slow one (method no.1) and a fast one (method no.2). These are described in Appendix C.

4.1.3 Stability Test

To assure the thermal stability of the HDPE at 190°C for the duration of the longest experiment (3 hours), a time-sweep of three hours (Table 4.1) was performed. Since the effects of degradation are more visible at low frequency, 0.05 rad/s was chosen. The strain applied was below the limit for linear viscoelasticity (≤20%), and the gap was set at 1mm. Time-sweeps were performed under an inert atmosphere (nitrogen gas) and also under an oxygen contaminated atmosphere. In the second case, the sample was heated and prepared under nitrogen. The flow of gas was then interrupted before beginning the time-sweep. If no degradation occurs, rheological properties (viscosity, storage and loss

moduli...) will stay constant. Since some experiments were also done for 20 minutes at 220°C (Section 4.3.4), we did a time-sweep at 220°C under nitrogen for 30 minutes.

TABLE 4.1 Time-sweep conditions.	
Temperature [°C]	190
Frequency [rad/s]	0.05
Strain [%]	10
Gap [mm]	1
Duration [hr]	3
N_2 [psi]	75-80
Sample preparation	Method no.1

4.1.4 Frequency Sweep

The dynamic moduli [$G'(\omega)$, $G''(\omega)$] for the HDPE were measured at 190 °C between 0.005 and 500 rad/s with an ascending frequency sweep test (Table 4.2). All experiments were conducted under an inert atmosphere (N_2) with a strain of 10%. A different sample was used for each experiment, since the stress history caused by a previous frequency sweep on the sample could influence the results. The samples were prepared according to method no.1 and trimmed at 1mm to obtain a flat edge (Figure 2.5).

TABLE 4.2 Frequency-sweep conditions.	
Temperature [°C]	190
Frequency [rad/s]	0.005 to 500
Strain [%]	10
Gap [mm]	1
Edge	flat
# points/decade	7
Duration [hr]	3
N_2 [psi]	75-80
Sample preparation	Method no.1

According to the accepted rule of thumb (for control charting of data containing Gaussian errors) the minimum number of runs required for a reliable estimate of population variation is 20. Since the coefficient of variation is needed to apply the linear regression with and without regularization, the average dynamic moduli as well as the standard deviation are based on 20 experiments. The standard deviation depends on the resin studied, the apparatus used, and, as we will see in Chapter 5, on the frequency. In the case of the average, assuming an average relative standard deviation of 7%, seven experiments would have been sufficient to correctly identify a difference of 10% in the means of two populations with a probability between 0.95 and 0.975.

4.2 STATISTICAL ANALYSIS[31]

Two types of error are encountered in experiments. The first, within sample error, is due to measurement noise (in this case the torque). The second one, between sample error, is due to variations in the gap or the sample diameter and will affect all the measurements on a given sample to the same extent. This last type of error will cause a shift in the viscosity curve of one sample compared to the next. To get rid of the between sample error, a correction factor ($\delta G(\omega_i)$) is introduced. The correction factor is calculated as follows:

$$\delta G_i(\omega) = \frac{G_i(\omega) - G_{avg}(\omega)}{G_{avg}(\omega)} \qquad 4.1$$

where $G_i(\omega)$ corresponds to $G'(\omega)$ or $G''(\omega)$, and $G_{avg.}(\omega)$ is the average value of G' or G'' for each frequency ω. These values of $\delta G_i(\omega)$ are then plotted as a function of the frequency (Figure 4.1). For each experiment, the value of $\delta G_i(\omega)$ reaches a plateau at a frequency ω^*. The correction factor (δG_i) will be the average value of $\delta G_i(\omega)$ for $\omega \geq \omega^*$. The corrected dynamic data sets are then calculated as follows:

$$G_{i_{corr}}(\omega) = \frac{G_i(\omega)}{1 + \delta G_i} \qquad 4.2$$

The average dynamic moduli [$G'(\omega)$, $G''(\omega)$], as well as the coefficient of variation, is then calculated using the values of G'_{corr} and G''_{corr}.

In addition to avoiding the problem of within sample error, this method of correction also provides a way to verify the quality of the results and a reliable criterion for discarding bad data sets. Section 5.2 will provide an example of this procedure.

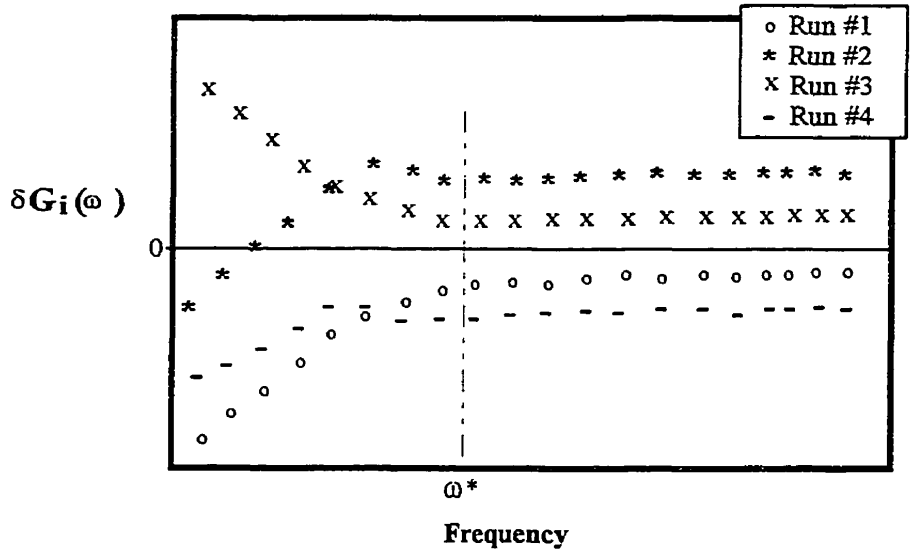

FIGURE 4.1 Variation of the corrected factor as a function of frequency.

4.3 IMPACT OF DATA ERRORS

The impacts of gap size, edge shape, residual stress due to the preparation of the sample and temperature were studied separately. This study is not exhaustive and is only a first step in the study of the impact of errors. This study is therefore qualitative. In each case (Sections 4.3.1 to 4.3.4), only 8 runs were conducted to obtain a reliable average. The average deviation was not needed in these cases. Also, the frequency range was restricted to 0.05 to 500 rad/s to avoid the time-consuming low frequencies (the duration of the experiment is reduced from 3 hours to 20 minutes). Table 4.3 presents the conditions for the reference state, and Table 4.4 presents the parameters studied independently for the impact of data errors.

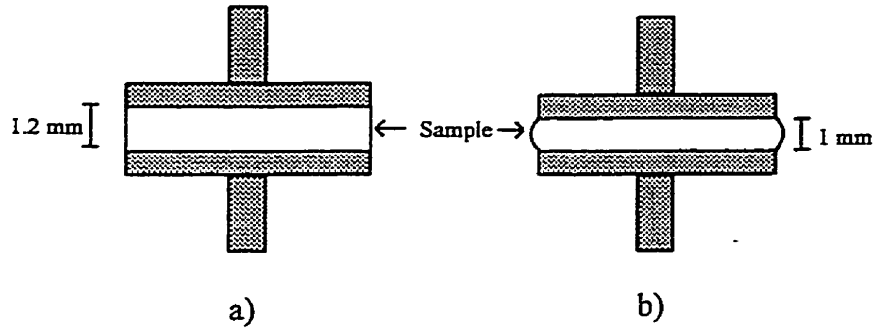

FIGURE 4.2 Obtaining of a cambered edge.

4.3.3 Impact of Residual Stresses

To study the residual stress, the samples were prepared according to method no.2 (Appendix C). This method does not allow the sample to relax as much as method no.1. All other parameters were as shown in Table 4.3.

4.3.4 Temperature Impact

To find the impact of temperature, 8 frequency sweeps were conducted at 220°C. All the other parameters were those shown in Table 4.3.

—CHAPTER 5—

5. EXPERIMENTAL RESULTS

5.1 STABILITY OF THE RESIN

Figure 5.1 presents the complex viscosity for the HDPE at 190°C and 220°C under nitrogen. It can be seen that the HDPE is stable for three hours at 190°C and for 30 minutes at 220°C (Table 4.1 and Section 4.1.3 give the experimental conditions). The complex viscosity at 190°C without nitrogen is also shown (190°C no N2). Under these conditions, degradation of the sample occurs very fast, and the complex viscosity is not constant. Degradation occurred before the first data point as the nitrogen flow was stopped, before the beginning of the frequency-sweep.

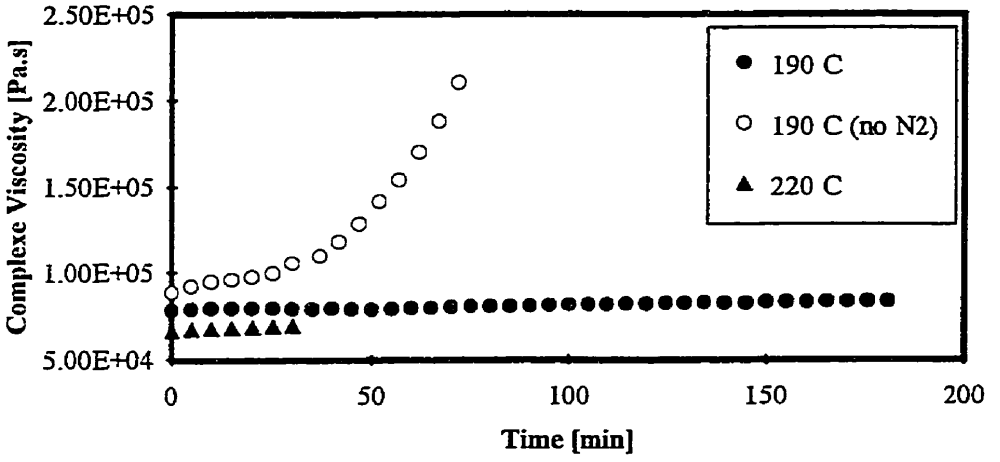

FIGURE 5.1 Time-sweep of HDPE at 190°C, with and without nitrogen.

5.2 FREQUENCY SWEEP

5.2.1 Dynamic Moduli

The 20 experiments were treated as explained in Section 4.3. The correction factor for G' and G'' (Equation 4.1) was calculated for each experiment. Figure 5.2 gives an example for G'' in the case of the first ten experiments. All other experiments showed similar results. A plateau was reached above 1rad/s, and the average correction factor was determined for $\omega \geq 5$rad/s.

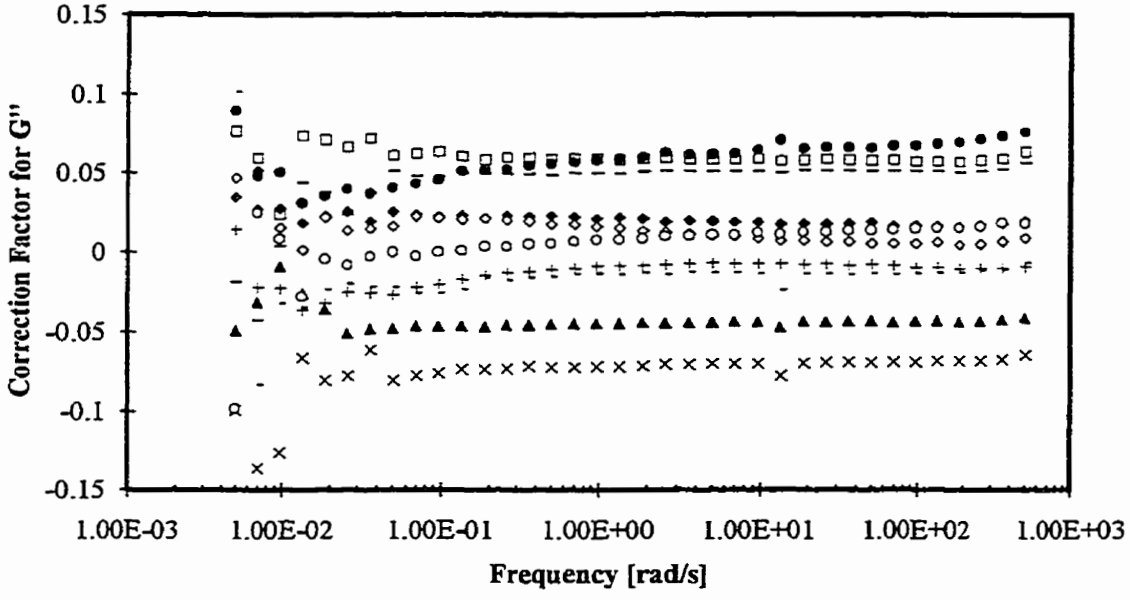

FIGURE 5.2 Correction factor of G'' for the first ten runs.

As was previously mentioned, the technique used to treat the data eliminates the between sample error and also permits the identification of unsatisfactory data sets. For example, Figure 5.3 presents the correction factor for G'' for the experiments 1, 2, 3, 8 and 13. With this method, it is possible to conclude that data from experiments 8 and 13 should be discarded. In fact, the correction factor does not reach a plateau at frequencies above 1rad/s for either runs 8 or 13. Such behavior can be caused by an air bubble trapped in the sample, degradation due to insufficient nitrogen flow, or incorrect trimming of the sample. In order to obtain twenty 'good' experiments, twenty-three experiments were

necessary. The average of the twenty experiments is presented by Figure 5.4 and Table D.1 in Appendix D.

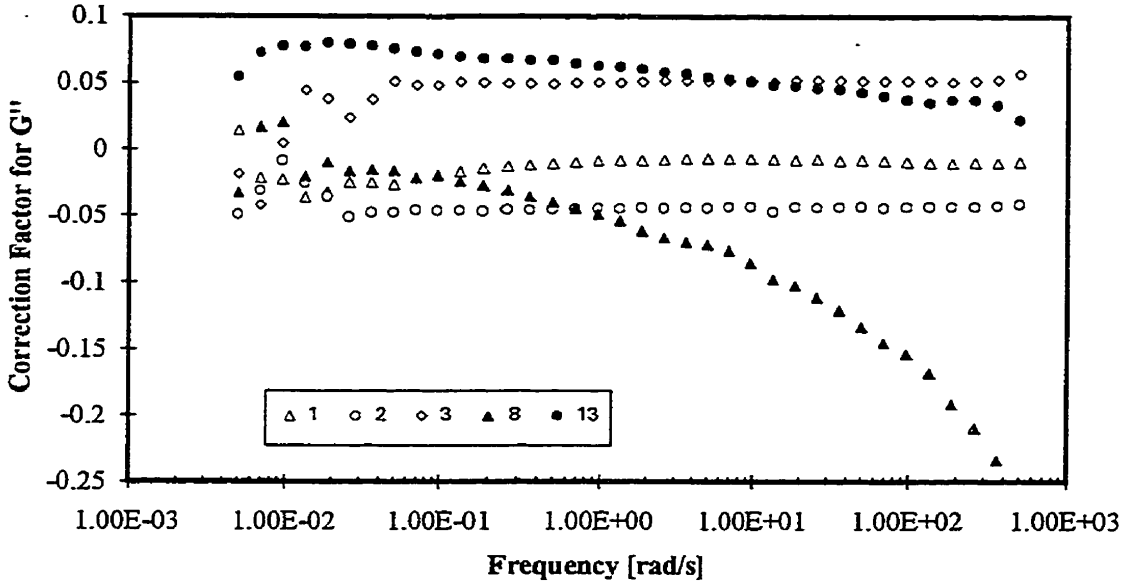

FIGURE 5.3 Correction factor of G'' for the experiments number 1, 2, 3, 8 and 13.

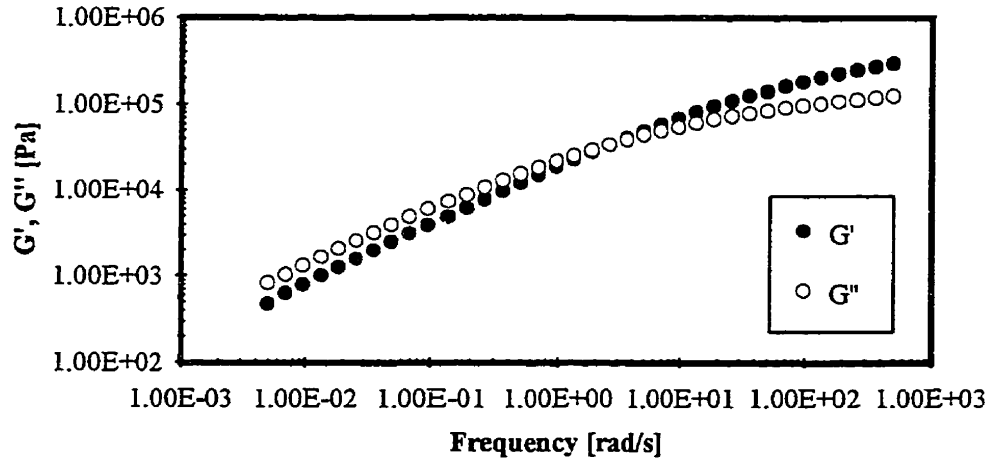

FIGURE 5.4 Dynamic moduli of HDPE.

5.2.2 Average Standard Deviation

Figure 5.5 shows the relative standard deviation as a function of frequency. The average relative standard deviation obtained was 1.86% for G' and 1.11% for G''. The average of these two values was 1.49%. Thus, the value used for the coefficient of variation in the linear regression with and without regularization was 0.015.

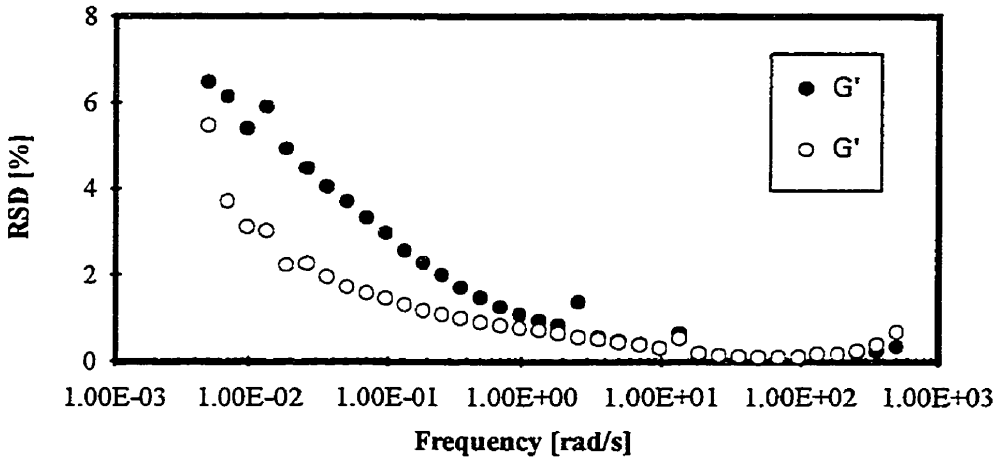

FIGURE 5.5 Relative standard deviation for the HDPE.

5.3 IMPACT OF DATA ERRORS

5.3.1 Gap Size Impact

Figure 5.6a presents the dynamic moduli resulting from a gap setting of 1.5mm with all other parameters as shown in Table 4.2. The increase of the gap results in a vertical shift of the dynamic moduli. Figure 5.6b gives the difference between these dynamic moduli and the reference data as a function of frequency. This difference is calculated as follows:

$$Diff = \left(\frac{G_{error} - G_{reference}}{G_{reference}} \right) \times 100 \qquad 5.1$$

where G is either G' or G''.

An average difference of 27% for both the storage and loss moduli corresponds to an increase of 50% in the gap. This large difference is not surprising, since it is known that the value of the gap has a large impact on the moduli.

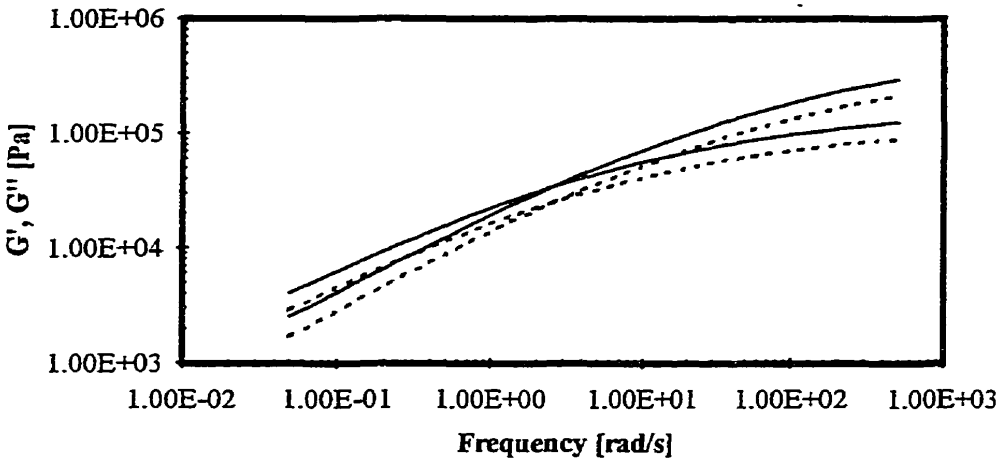

FIGURE 5.6a Dynamic moduli for the gap of 1.5mm (——). Reference data (——).

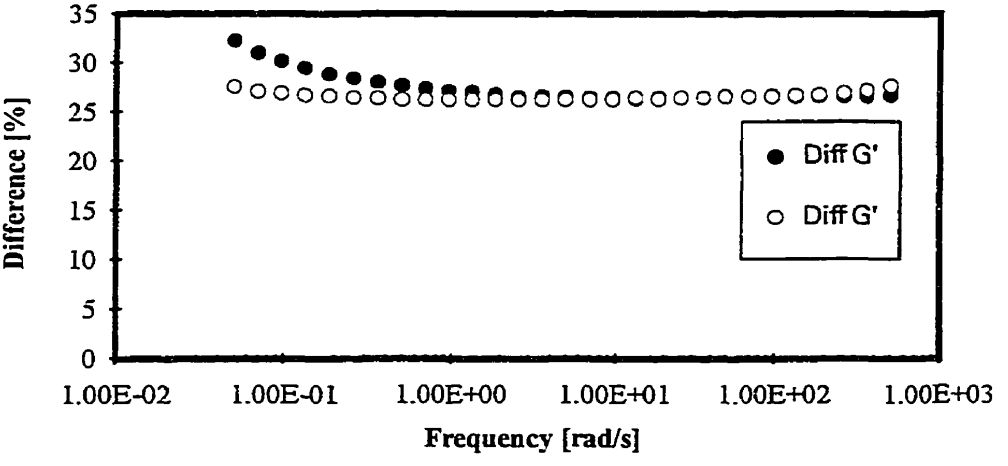

FIGURE 5.6b Difference between the dynamic moduli for the gap of 1.5mm and the dynamic moduli for the reference data.

Depending the purpose of the rheological measurements, both shapes (flat and cambered) may be appropriate. If the purpose is the comparison of rheological properties between resins, as long as the same shape is used for all samples, the edge shape does not matter. Often flat edges are preferred because this technique is supposed to give better reproducibility.

5.3.3 Impact of Residual Stresses

Figure 5.8a gives the dynamic moduli when the samples were prepared using method no.2 (high residual stresses). In this case, the data are shifted horizontally, and the impact appears to be a function of frequency. Figure 5.8b gives the difference between these dynamic moduli and the reference data. The difference in the storage modulus starts at 16% and decreases to 4%, giving an average of 8%, and the difference in the loss modulus starts at 10% and decreases to 2%, giving an average of 5%. This is probably due to the fact that the residual stresses are decreasing with time, bringing the sample closer to the reference data as time passes. Therefore it is likely that the impact of residual stresses in the sample is a function of the amount of time that has passed since the experiment started rather than the frequency at which the measurement is being taken.

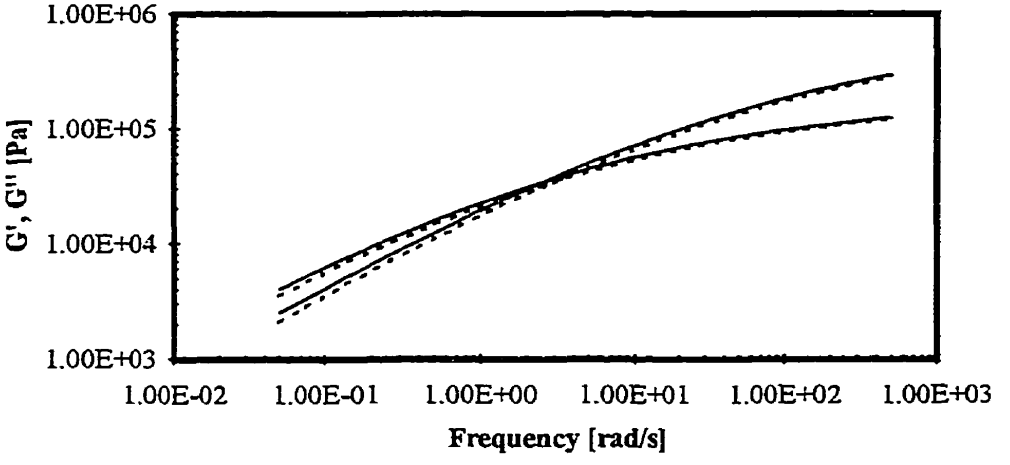

FIGURE 5.8a Dynamic moduli for high residual stresses (——). Reference data (——).

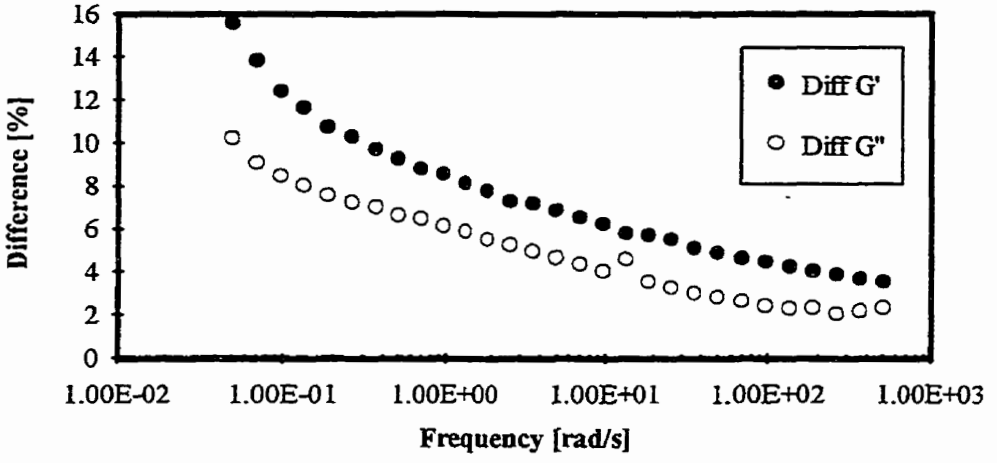

FIGURE 5.8b Difference between the dynamic moduli for high residual stresses and the dynamic moduli for the reference data.

5.3.4 Temperature Impact

Figure 5.9a gives the dynamic moduli at 220°C. In that case also, the data are horizontally shifted, and the impact decreases with increasing frequency. Figure 5.9b gives the difference as a percentage (Equation 5.1). The difference in the storage modulus starts at 34% and decreases to 10%, giving an average of 21%, and the difference in the loss modulus starts at 27% and decreases to 3%, giving an average of 14%. Therefore we can conclude that temperature has a larger impact at low frequency and that the impact decreases as the frequency increases.

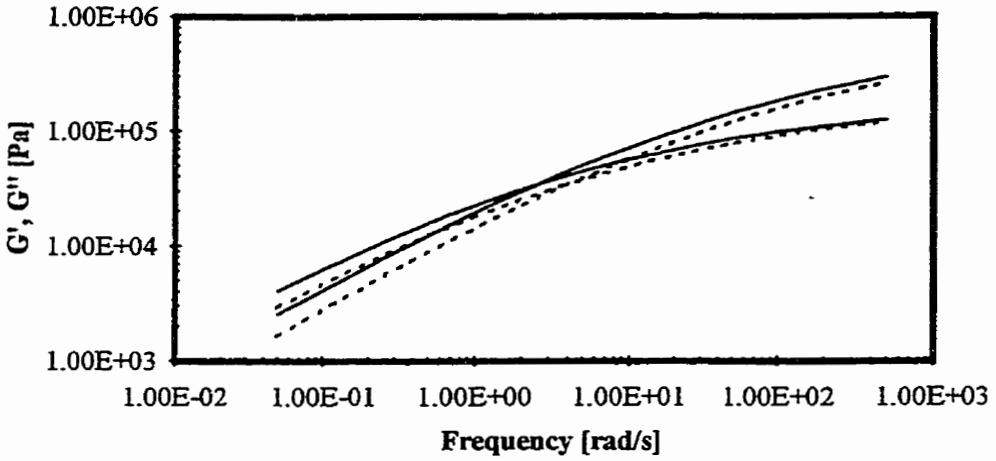

FIGURE 5.9a Dynamic moduli at 220°C (-----). Reference data (——).

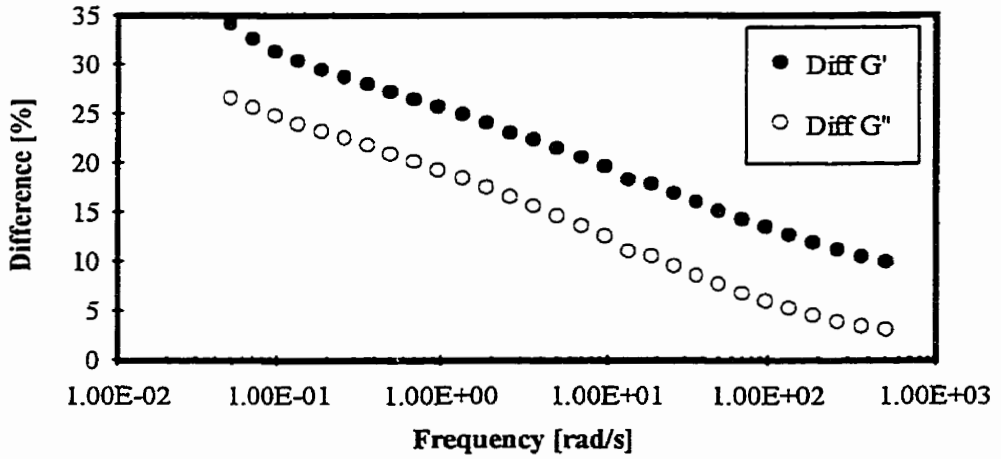

FIGURE 5.9b Difference between the dynamic moduli at 220°C and the dynamic moduli for the reference data.

—CHAPTER 6—

6. ANALYSIS OF THE DATA

6.1 COMPARISON OF METHODS FOR DETERMINING THE SPECTRUM

6.1.1 Determination of the Spectrum

In the case of the linear regression method, the relaxation spectrum is determined by trial and error. The best solution is determined by trying different numbers of relaxation times (N) and by inspecting the average absolute deviation (|AD|) as well as the standard error in G_i ($\sigma^2(G_i)$, Equation 2.27). When different ranges of relaxation times ($\lambda_{min.}$, $\lambda_{max.}$) were tried, the standard error on G_i was found to be large if $\lambda_{min.}$ was less than $1/\omega_{max.}$ or $\lambda_{max.}$ was greater than $1/\omega_{min.}$. Thus, the relaxation times always correspond to the frequency range ($\lambda_{min.}=1/\omega_{max.}$ and $\lambda_{max.}=1/\omega_{min.}$). Also, as described in Chapter 2 and references [17, 25], as N increases, negative G_i start to appear and the standard error for G_i increases. The number of relaxation times should stay small.

In the case of the linear regression with regularization, the spectrum is insensitive to the number of relaxation times, and a large value of N can be introduced [17]. The number of relaxation times per decade was arbitrarily set for the whole study of each dynamic moduli. This number was set at 6 points per decade for the simulated data and 10 points per decade for the polybutadiene. These values are the same as those used by Orbey and Dealy [25]. For the HDPE and the polybutadiene samples, it was necessary to divide the values of G' and G'' by 10^6 in the calculation of the regularization parameter, to prevent a machine precision limit. This problem occurs when the condition number (ratio of the largest, in magnitude, of the singular value to the smallest of the singular value) is too large [26].

Finally, the nonlinear regression method does not require any input data other than the dynamic moduli values. The software adjusts the number of relaxation times and their

N=6. With the linear regression with regularization (LRwR), it is possible to recover very closely the original spectrum with a large number of relaxation times (N=30 and λ^*=2.17). The nonlinear regression method (IRIS) gives results that fall on the original spectrum for N=6.

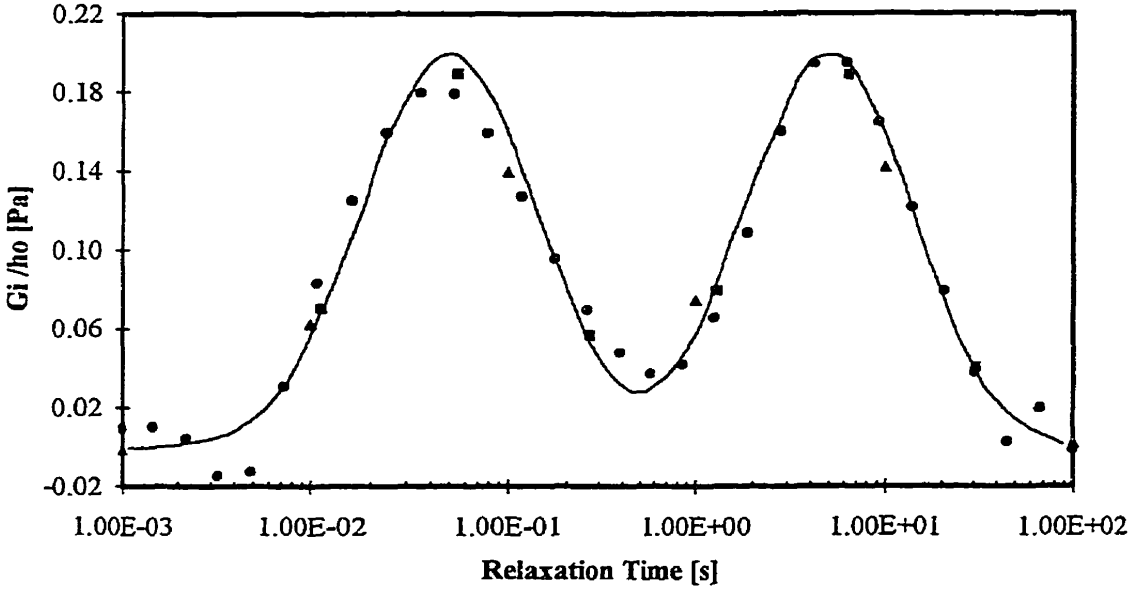

FIGURE 6.1 Comparison of the three methods used to infer the relaxation spectrum of simulated data (— original spectrum).
● LRwR (λ^*=2.17 and h_0=0.397) ▲ LR (h_0=2.30) ■ IRIS (h_0=1.58).

The comparison of the spectra obtained with the linear regression and the nonlinear regression using the dynamic data for the HDPE is shown in Figure 6.2. The relaxation spectrum was obtained for N=5 with the linear regression method. The nonlinear regression method gives results with N=8. Unfortunately, the spectrum of the HDPE could not be determined for a large number of relaxation times since it was not possible to regularize the solution for that particular set of dynamic moduli. This problem will be discussed in detail in Section 6.3.2. Although it is not possible in this case to compare with the "true" spectrum, it is possible to say that the two spectra agree reasonably well.

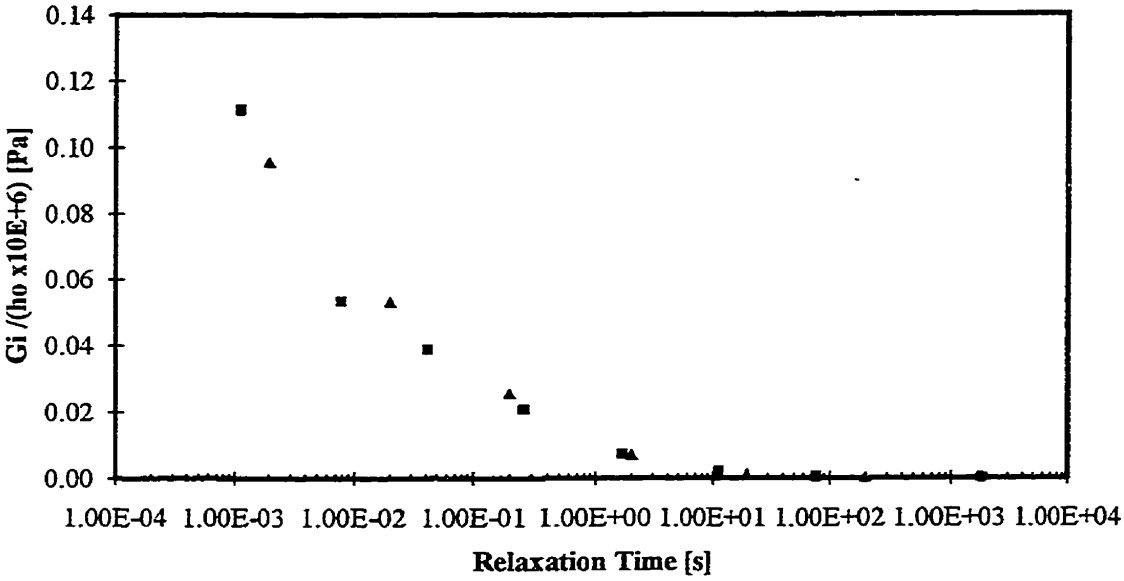

FIGURE 6.2 Comparison of the two methods used to infer the relaxation spectrum of HDPE.

▲ LR (h_0=2.30) ■ IRIS (h_0=2.04).

The results obtained for the polybutadiene are compared in Figure 6.3. The linear regression method gives positive G_i values with N=4. With the linear regression with regularization , it is possible to infer the spectrum for N=30 (λ^*=0.916). In that case, as was shown by Orbey and Dealy [25], it is possible to use relaxation times outside the frequency range. The spectrum was calculated for $\lambda_{min.}=1x10^{-5}$ instead of $1x10^{-3}$ ($1/\omega_{max.}$). The nonlinear regression method gives results for N=3. All the results seem to agree reasonably well, as in the case of the HDPE.

The dynamic moduli were then recalculated from the discrete spectra given in Figures 6.1, 6.2 and 6.3. The absolute average deviations between the experimental and recalculated moduli are listed in Table 6.1 for the three methods and the three data sets. The regularization method gives the smallest average deviation in G' and G''. The nonlinear regression method gives the best results if a small number of relaxation times are desired. The linear regression gives the poorest results. These conclusions are in agreement with those of Orbey and Dealy [25].

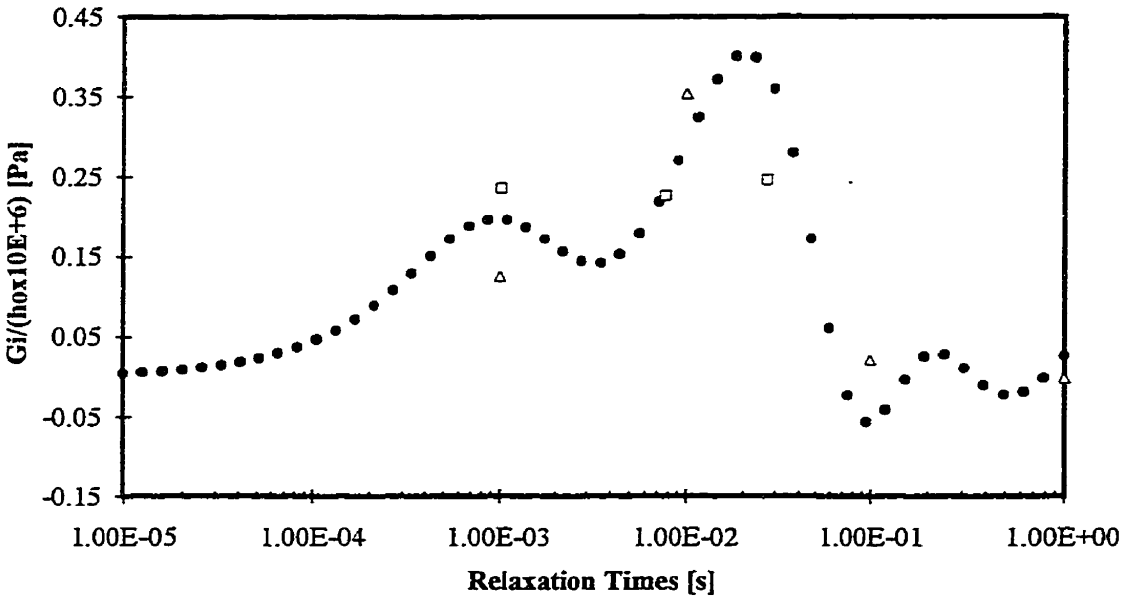

FIGURE 6.3 Comparison of the three methods used to infer the relaxation spectrum of polybutadiene.

● LRwR (λ^*=0.916 and h_0=0.235) Δ LR (h_0=2.30) □ IRIS (h_0=1.64).

TABLE 6.1 Values of the absolute average deviation for recalculated dynamic moduli.

Method	|AD| G'	|AD| G''
Polybutadiene		
LR	16.67	13.74
LRwR	0.75	0.91
IRIS	1.18	1.27
HDPE		
LR	2.85	3.46
IRIS	1.48	1.19
Simulated Data		
LR	6.20	9.94
LRwR	3.01	4.12
IRIS	3.12	4.37

6.2 IMPACT OF DATA POINT DENSITY

The next three figures present the impact of point density on the discrete spectrum of polybutadiene for the three methods. The original dynamic moduli (17 data points over 3 decades) contain 6 points per decade (Figure 3.4). To study the impact of point density, a certain number of points per decade was deleted, reducing the number to 3 and 2 points per decade. The spectra of these two smaller data sets were then inferred using the three methods and compared to the spectrum obtained for the original data set. Figure 6.4 presents the results for the linear regression (LR). The spectrum inferred with the regularization method for the data set with 6 points per decade is shown as a reference. Figure 6.5 presents the results of the regularization method (LRwR) and Figure 6.6 gives the results for the nonlinear method (IRIS). We see that the spectrum is nearly unchanged for linear regression with regularization. Although there is a significant effect in the case of the one calculated using nonlinear regression, even here the effect is small. The same type of results were obtained for the HDPE data and the simulated data.

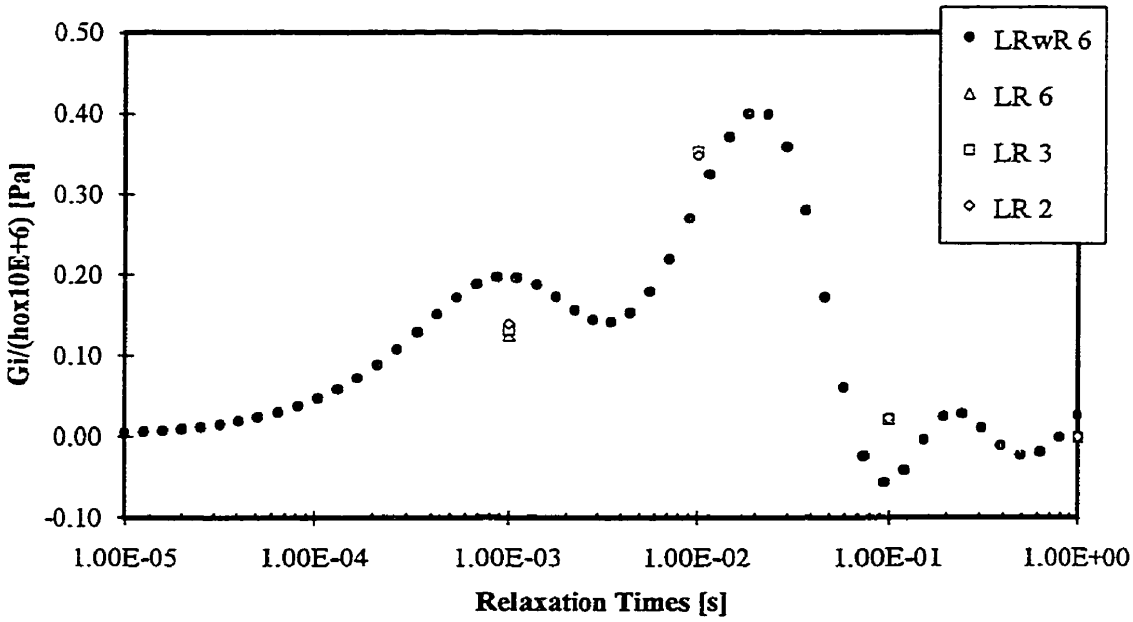

FIGURE 6.4 Impact of point density on the relaxation spectrum of polybutadiene (LR).

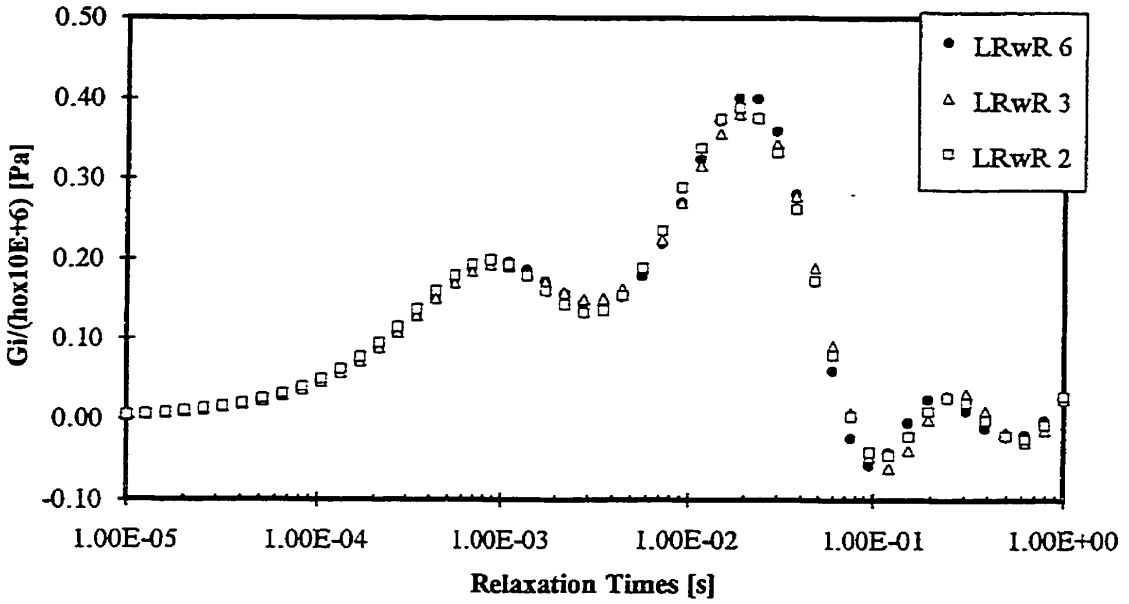

FIGURE 6.5 Impact of point density on the relaxation spectrum of polybutadiene (LRwR).

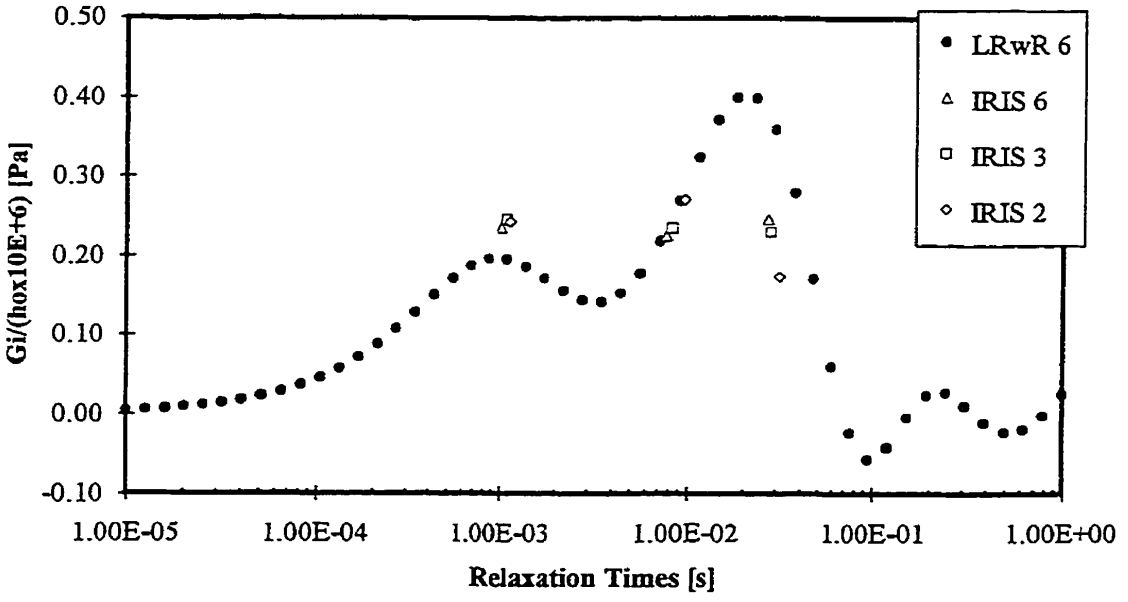

FIGURE 6.6 Impact of point density on the relaxation spectrum of polybutadiene (IRIS).

TABLE 6.3 Impact of point density on the absolute average deviation for recalculated dynamic moduli of HDPE.			
Method	**Points/decade**	**|AD| G'**	**|AD| G''**
LR	7	2.83	3.41
	4	2.93	3.40
	3	2.93	3.39
	2	3.11	3.39
IRIS	7	1.48	1.19
	4	1.46	1.06
	3	1.44	1.10
	2	1.58	1.20

TABLE 6.4 Impact of point density on the absolute average deviation for recalculated dynamic moduli of simulated data.			
Method	**Points/decade**	**|AD| G'**	**|AD| G''**
LR	5	6.21	9.95
	3	6.31	10.06
	2	6.19	10.01
LRwR	5	3.01	4.12
	3	3.47	4.28
	2	3.18	4.80
IRIS	5	3.12	4.37
	3	3.98	4.73
	2	5.27	5.69

6.3 IMPACT OF TIME-SCALE TRUNCATION

To study truncation, the dynamic moduli of the various data sets were truncated at low frequency, at high frequency and at both ends. Figure 6.7 gives two examples of truncated dynamic moduli in the case of the simulated data. The number in parenthesis refers to the number of data points deleted (multiple of the number of points per decade). For example, the data set (5/0) has only one decade deleted (5 data points) at low

frequency and the data set (10/5) has two decades deleted (10 data points) at low frequency and one decade deleted (5 data points) at high frequency.

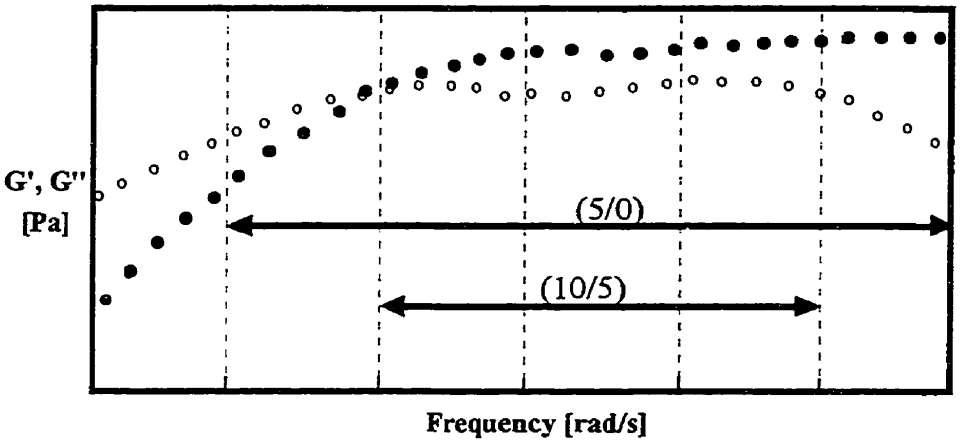

FIGURE 6.7 Examples of truncated dynamic moduli.

Using the three mathematical methods, the discrete linear spectra were calculated, and using the inferred spectra, the dynamic moduli were back-calculated. An average deviation was calculated for each truncated data set.

6.3.1 Simulated Spectrum

LINEAR REGRESSION

In the case of the simulated data, it was possible to compare the results to the "true" values (simulated relaxation spectrum). The data set was truncated at high frequency and at low frequency (1, 2, 3 and 4 decades were successively deleted in each case). Truncation was also done at both ends. Each decade contains 5 points.

Figures 6.8 to 6.10 present the relaxation spectra inferred using linear regression (LR) for truncation at high frequency, low frequency and both ends, for the simulated dynamic moduli. All the resulting spectra agree reasonably well with the "true" spectrum. Of course, the higher the number of truncated decades, the more distant the inferred

spectrum is from the true spectrum. This is especially true in the case of truncation at low frequency [(15/0) and (20/0)]. Truncation at both ends is consistent with the other results and seems to be simply the equivalent of an addition of the separate effects of truncations at high and low frequencies.

Each time the dynamic modulus data set is truncated, information is lost (for example $\omega_{max.}$ decreases). At the same time, the range of resulting relaxation times also decreases ($\lambda_{min.}=1/\omega_{max.}$). The result is that the spectrum extracted from the truncated dynamic data seems to contain sufficient information within the relaxation time range of the inferred spectrum.

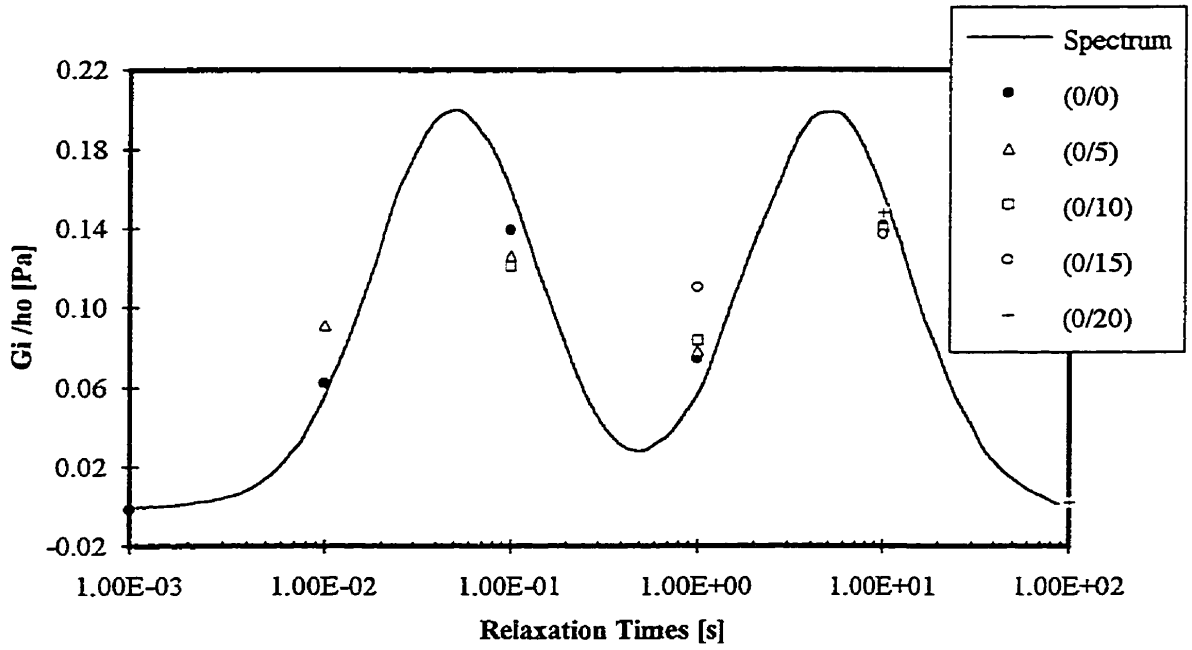

FIGURE 6.8 Impact of time-scale truncation at high frequency on the discrete spectrum of simulated data (LR). Original spectrum (——).

Figures 6.11 to 6.13 compare the recalculated dynamic moduli with the original moduli. As was seen with the spectrum, the recalculated moduli are in very good agreement with the original moduli, within the truncated range of frequency. But in most of the cases, the moduli are not properly recovered outside this range, as has been previously demonstrated [16]. In the case of simulated data, this was true for linear regression with and without regularization and also for nonlinear regression.

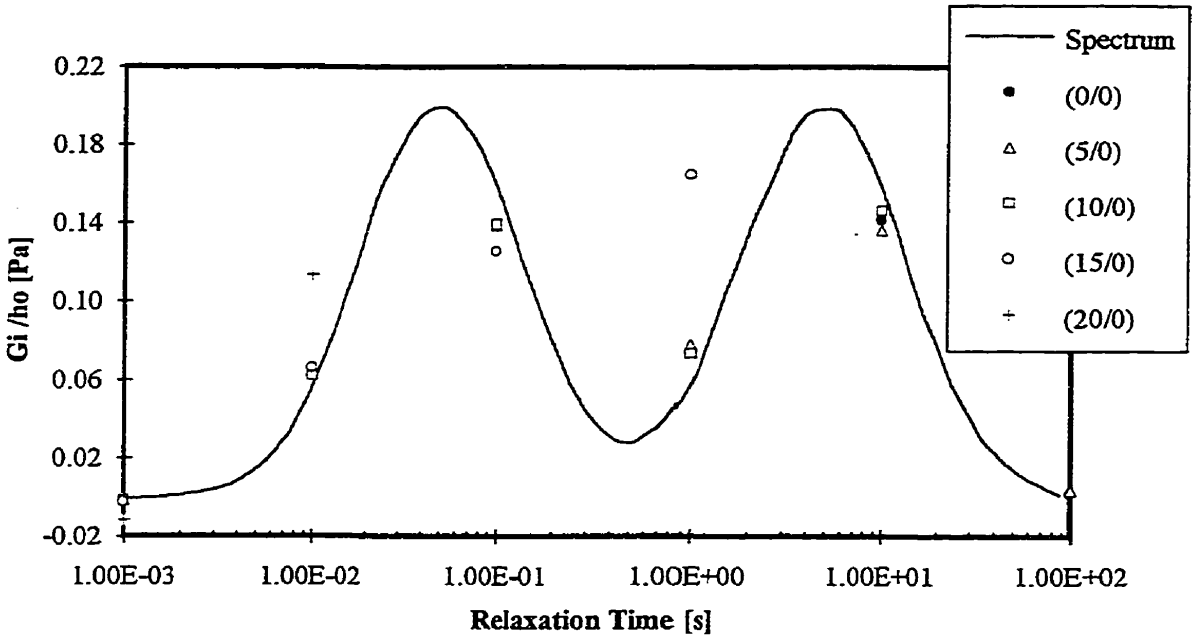

FIGURE 6.9 Impact of time-scale truncation at low frequency on the discrete spectrum of simulated data (LR). Original spectrum (——).

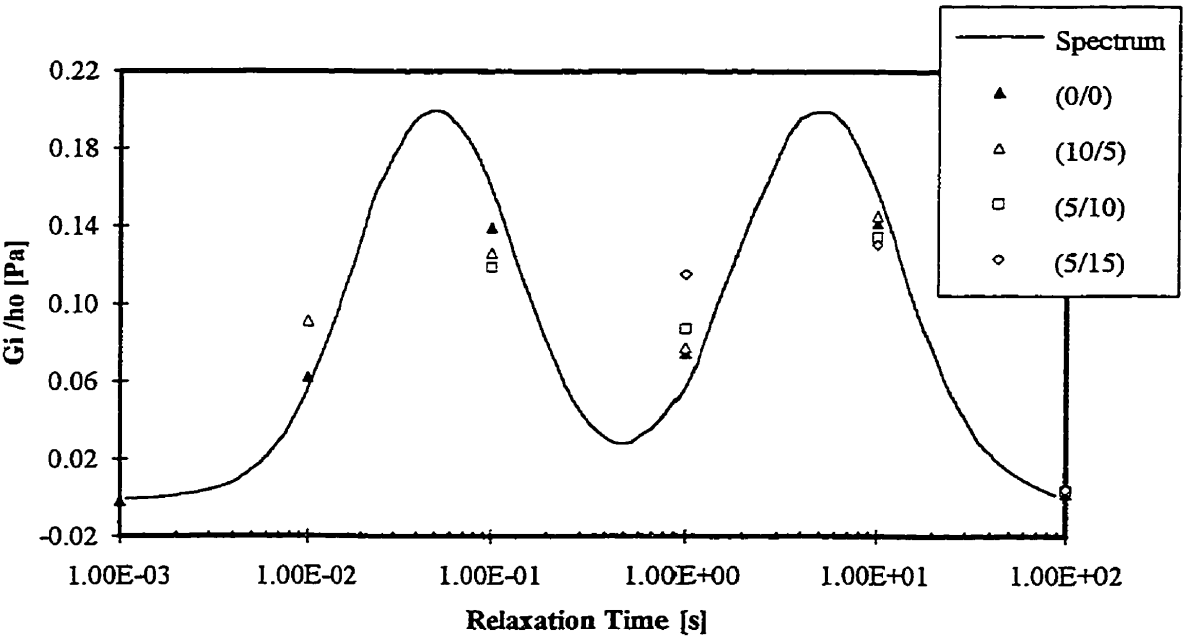

FIGURE 6.10 Impact of time-scale truncation at both ends on the discrete spectrum of simulated data (LR). Original spectrum (——).

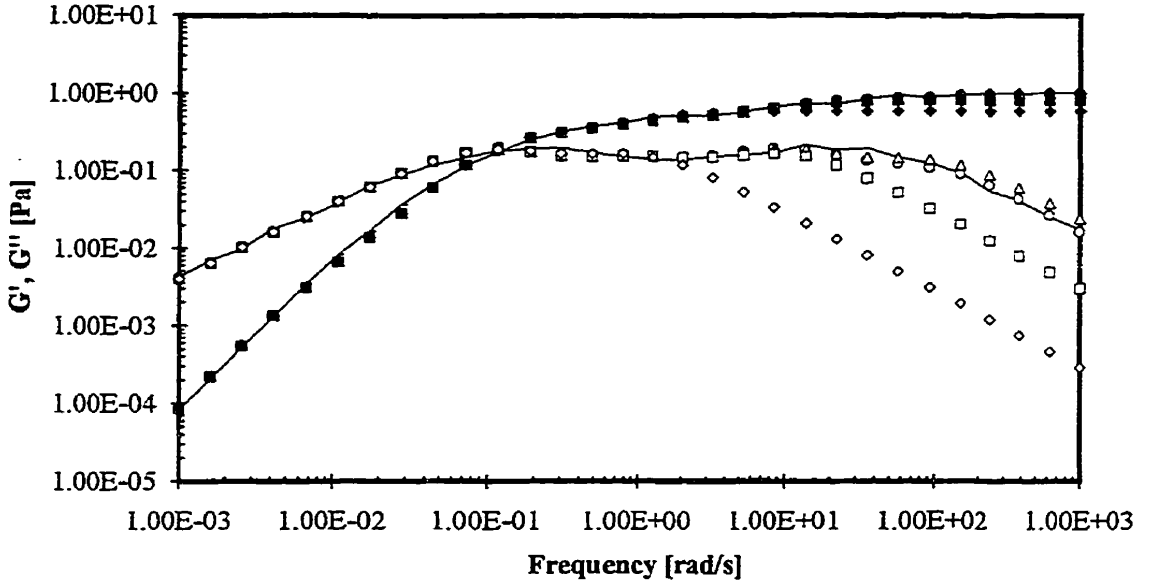

FIGURE 6.11 Impact of time-scale truncation at high frequency on the recalculated moduli using the spectrum of Figure 6.8 (—— =original spectrum).

●G' (0/0) ▲ G' (5/0) ▣ G' (10/0) ⊠ G' (15/0) ○ G'' (0/0) △ G'' (5/0) □ G'' (10/0) ◊ G'' (15/0).

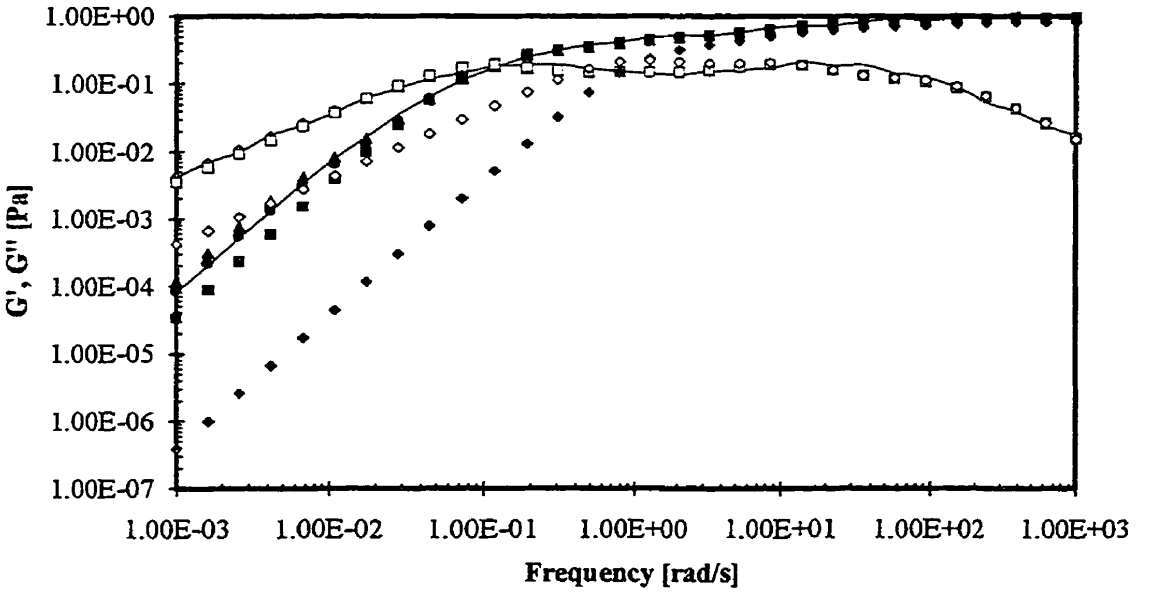

FIGURE 6.12 Impact of time-scale truncation at low frequency on the recalculated moduli using the spectrum of Figure 6.9. Original spectrum (——).

●G' (0/0) ▲ G' (0/5) ▣ G' (0/10) ⊠ G' (0/15) ○ G'' (0/0) △ G'' (0/5) □ G'' (0/10) ◊ G'' (0/15).

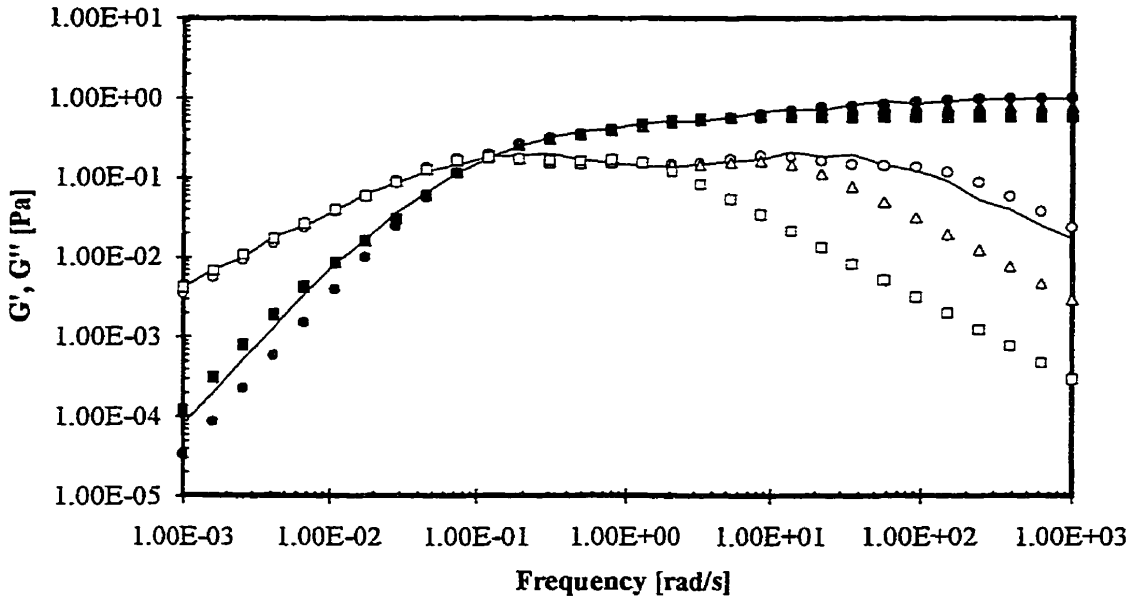

FIGURE 6.13 Impact of time-scale truncation at both ends on the recalculated moduli using the spectrum of Figure 6.10. Original spectrum (——).
●G' (10/5) ▲ G' (5/10) ▣ G' (5/15) ○ G'' (10/5) △ G'' (5/10) □ G'' (5/15).

Table 6.5 summarizes the behavior of the absolute average deviation between the recalculated moduli (using the spectra of Figures 6.8 to 6.10) and the original moduli without truncation. Table E.2 in Appendix E gives the numerical values of the average deviation. As is expected, the absolute deviation increases as the number of truncated decades increases. For truncation at high frequency, the average deviation of G'' was always found to be higher than that of G'. In the case of truncation at low frequency, we have the opposite situation, and the average deviation of G' is always found to be higher. For truncation at both ends, the results are consistent with the previous cases. For example, Table E.2 indicates an AD of 15.01 for G'' and 6.38 for G' for truncation at high frequency. The lost modulus is more affected. At low frequency, the average deviation is 9.86 for G'' and 11.43 for G'. This time the value is higher for G'. For truncation at both ends, it is a mix of the previous results, with 11.62 for G' and 15.01 for G''. This behavior was noted for all the methods and all the truncated data sets (simulated data, HDPE and polybutadiene).

TABLE 6.5 Summary of the impact of truncation on the absolute average deviation for recalculated dynamic moduli of simulated data (LR).	
Truncation	**|AD| G' and |AD| G''**
Truncation at high ω	|AD| ↗ as truncation ↗
Truncation at low ω	|AD| ↗ as truncation ↗
Truncation at both ends	Consistent

LINEAR REGRESSION with REGULARIZATION

Figures 6.14 to 6.16 present the relaxation spectra inferred using linear regression with regularization (LRwR) for truncation at high frequency, low frequency and at both ends. The spectra agree reasonably well with the "true" spectrum except at the smallest relaxation times when there is truncation of more than one decade at high frequency (0/10), (0/10) and (5/10).

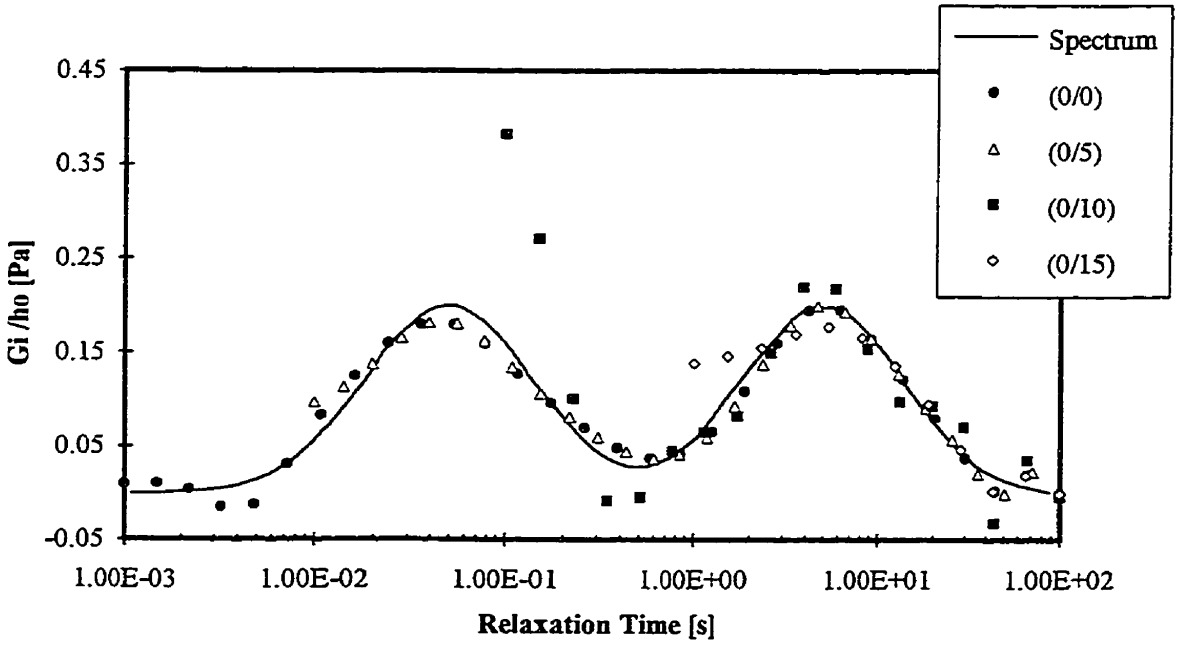

FIGURE 6.14 Impact of time-scale truncation at high frequency on the discrete spectrum of simulated data (LRwR). Original spectrum (——).

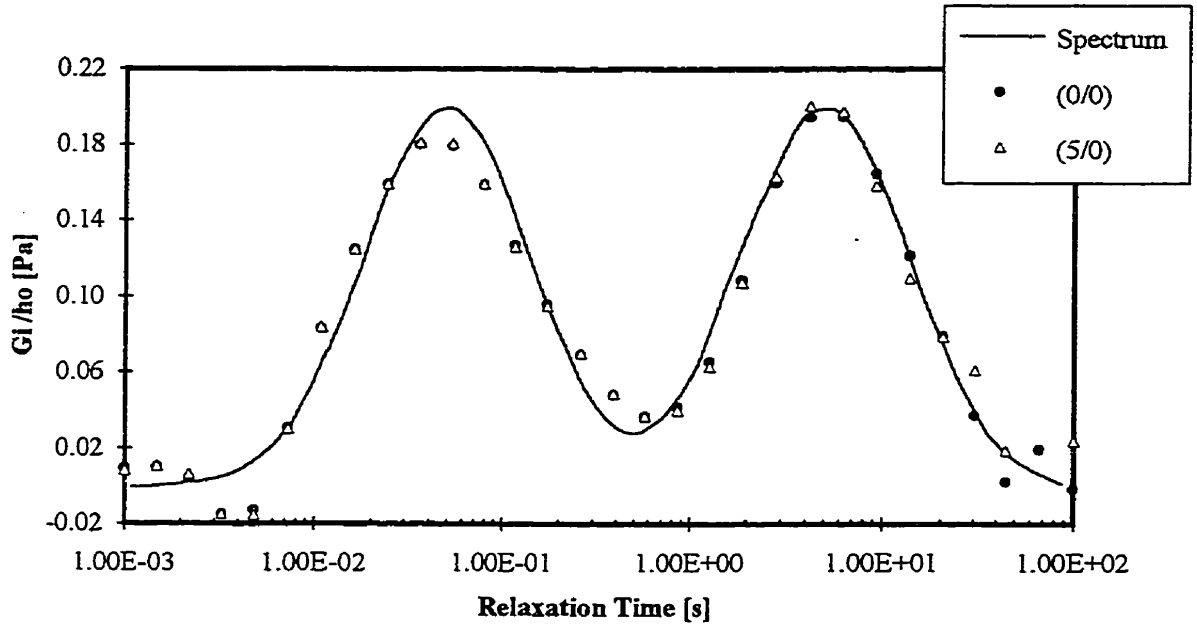

FIGURE 6.15 Impact of time-scale truncation at low frequency on the discrete spectrum of simulated data (LRwR). Original spectrum (——).

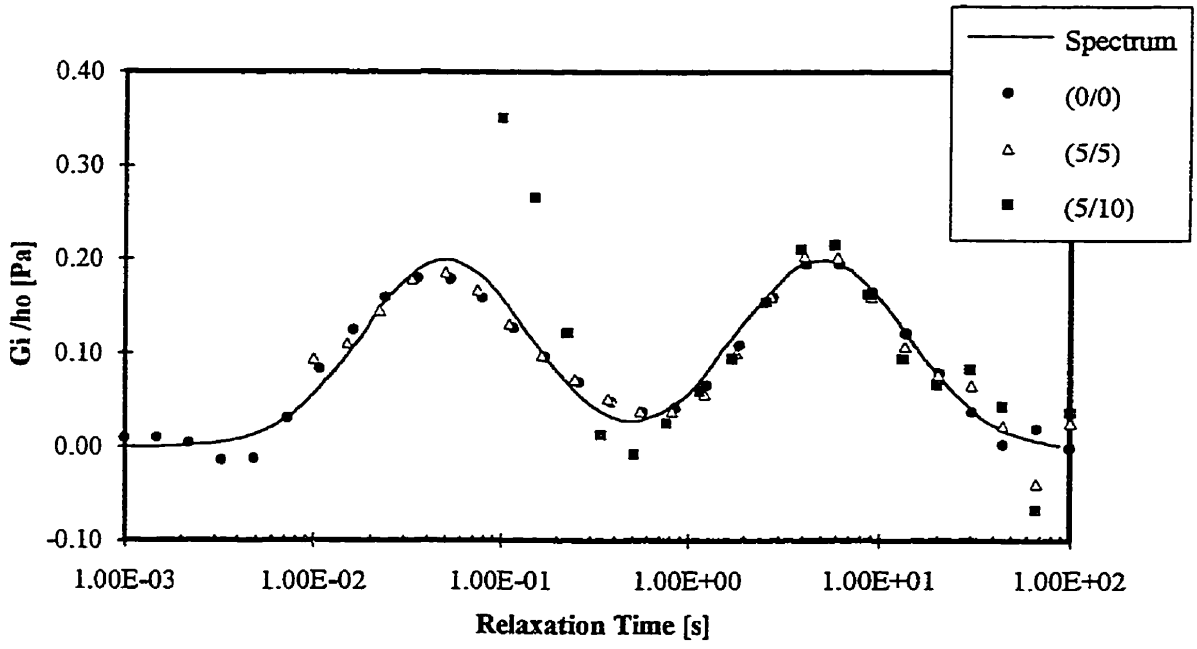

FIGURE 6.16 Impact of time-scale truncation at both ends on the discrete spectrum of simulated data (LRwR). Original spectrum (——).

Table 6.6 summarizes the behavior of the absolute average deviation between the recalculated moduli (using spectra of Figures 6.14 to 6.16) and the original moduli without truncation. Table E.3 in Appendix E gives the numerical values of the average deviation, and Table E.4 gives the regularization parameter. As expected, the absolute deviation increases as the number of truncated decades increases. For truncation at both ends, the results are consistent with the previous results.

TABLE 6.6 Summary of the impact of truncation on the absolute average deviation for recalculated dynamic moduli of simulated data (LRwR).

Truncation	|AD| G' and |AD| G''
Truncation at high ω	|AD| ↗ as truncation ↗ Not possible to regularize (0/20)
Truncation at low ω	|AD| ↗ as truncation ↗ Regularize only for (5/0)
Truncation at both ends	Consistent

It was not possible to regularize the moduli with 4 truncated decades at high frequency (0/20) or with more then 1 truncated decade at low frequency [(10/0), (15/0), (20/0)]. It was also not possible to regularize the following sets: (10/10), (10/5) and (10/15). In these cases, the regularization parameter was very small. If the regularization parameter is too small, it does not have any impact on the values of **W** (the singular values), and Equation 2.30 is reduced to Equation 2.26:

$$G_i = \sum_{k=1}^{N} \frac{W_{kk}}{W_{kk}^2 + \lambda^*} V_{ik} (U_k \cdot \mathrm{b}) \qquad 2.30$$

$$\frac{W_{kk}}{W_{kk}^2 + \lambda^*} \approx \frac{1}{W_{kk}} \qquad 6.3$$

$$G_i = \sum_{k=1}^{N} \frac{1}{W_{kk}} V_{ik} (U_k \cdot b) \qquad 2.26$$

We then go back to a simple linear regression method (Equation 2.26), and many negative values of G_i appear since N is large. This problem was previously encountered by Orbey and Dealy [25].

To understand why the dynamic moduli of the simulated data cannot always be regularized, we need to look at the complex viscosity for that data set (Figure 6.17). It appears that the plateau at low frequency contains essential information for the regularization method. Thus, as soon as the plateau at low frequency is truncated [(10/0), (15/0) and (20/0)], the data cannot be regularized properly. Also, if only the data points of the plateau are used (0/20), there is not sufficient information to find a good regularization parameter. Similar results will be given in the section about HDPE (Section 6.3.2).

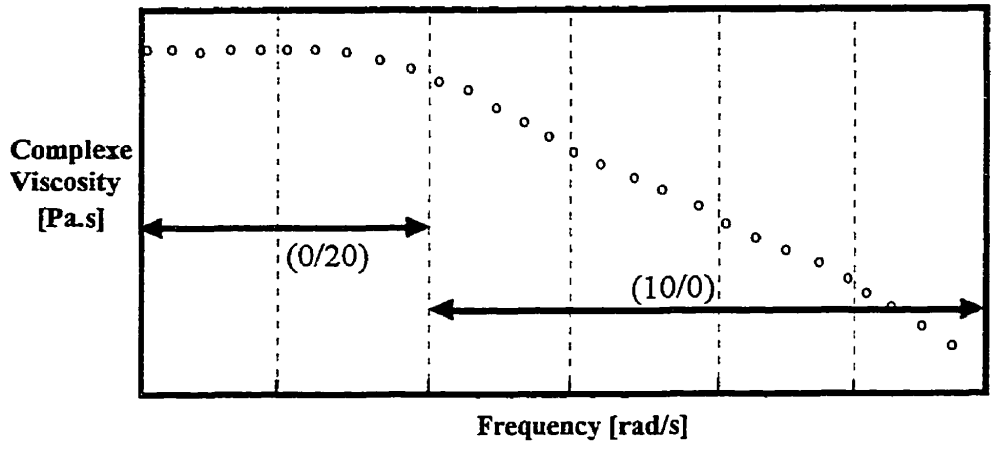

FIGURE 6.17 Complex viscosity versus frequency for the simulated spectrum.

NONLINEAR REGRESSION

Figures 6.18 to 6.20 give the discrete spectrum inferred using nonlinear regression (IRIS) for truncation at high frequency, low frequency and both ends. The results are not as good as those for the other two methods, especially at low frequency, but the spectrum is reasonably well recovered.

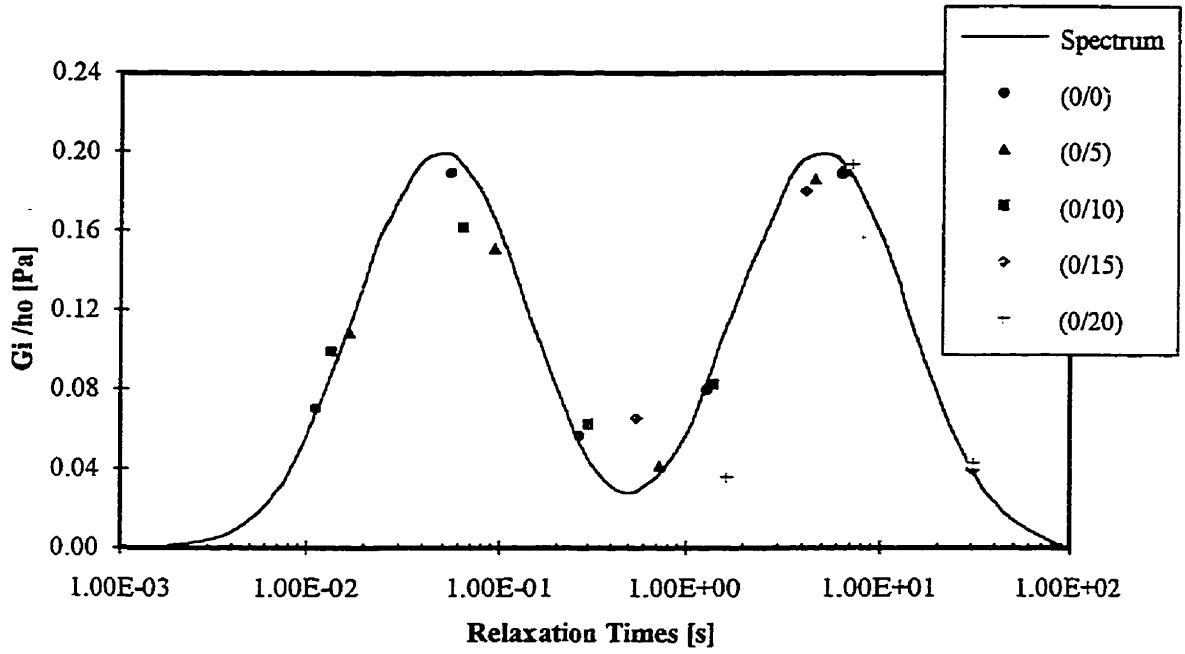

FIGURE 6.18 Impact of time-scale truncation at high frequency on the discrete spectrum of simulated data (IRIS). Original spectrum (——).

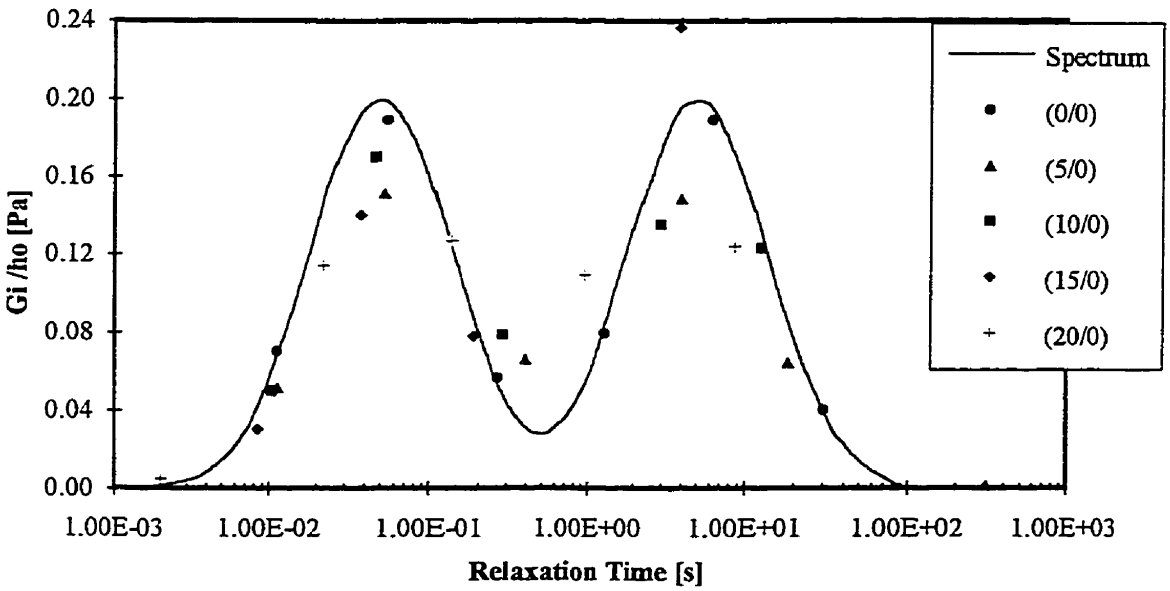

FIGURE 6.19 Impact of time-scale truncation at low frequency on the discrete spectrum of simulated data (IRIS). Original spectrum (——).

6.3.2 HDPE

LINEAR AND NONLINEAR REGRESSIONS

For the HDPE, there is no "true" spectrum. We considered the (0/0) spectrum as the reference case since according to the previous results, it is very close to the "true" spectrum. The data set was truncated at high frequency and at low frequency (1, 2, and 3 decades were successively truncated). It was also done at both ends. Each decade contains 7 points.

Figure 6.21 presents the relaxation spectrum inferred with the linear regression (LR) for truncation at high frequency of the HDPE dynamic moduli. The spectra agree reasonably well with the (0/0) spectrum in the case of the linear regression. Of course the higher the number of deleted decades, the further the inferred spectrum is from the reference spectrum (0/0). In the case of the nonlinear regression (IRIS), the deviation from the reference case was larger (Figure 6.22).

The recalculated dynamic moduli were compared in all the cases (linear regression and nonlinear regression) with the original moduli. The recalculated moduli were in very good agreement with the original data, within the truncated range of frequency. In most of the cases, the moduli are not properly recovered outside this range, as was previously demonstrated [16].

Table 6.8 summarizes the behavior of the absolute average deviation between the recalculated moduli and the original moduli without truncation (Tables E.6 and E.7 give the numerical values of the average deviation). As expected, the absolute deviation increases as the number of truncated decades increases both with the linear and nonlinear regressions.

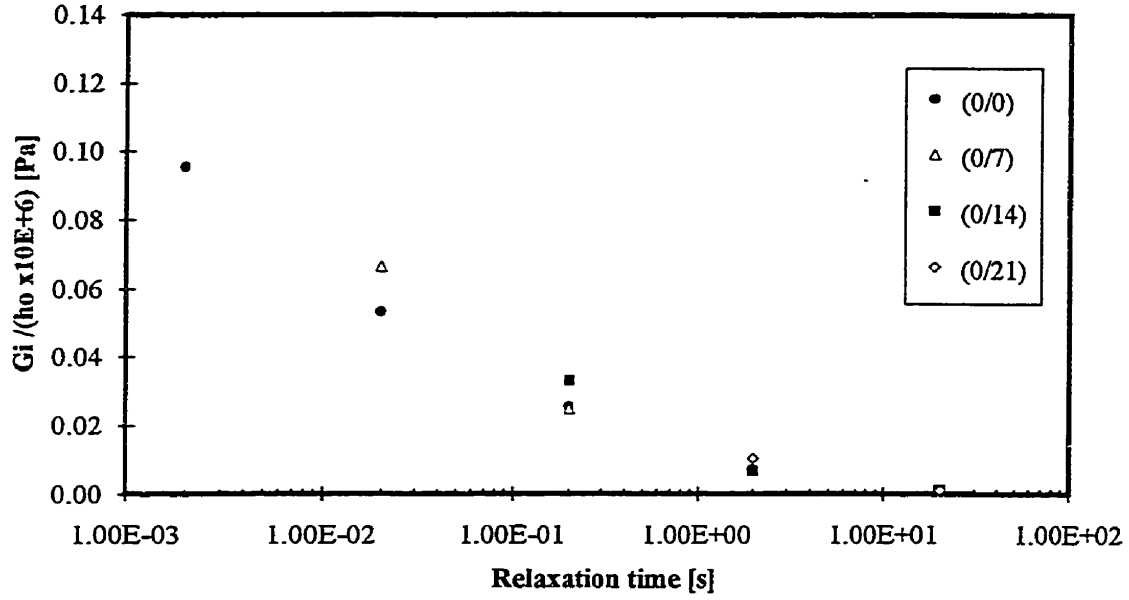

FIGURE 6.21 Impact of time-scale truncation at high frequency on the discrete spectrum of HDPE (LR).

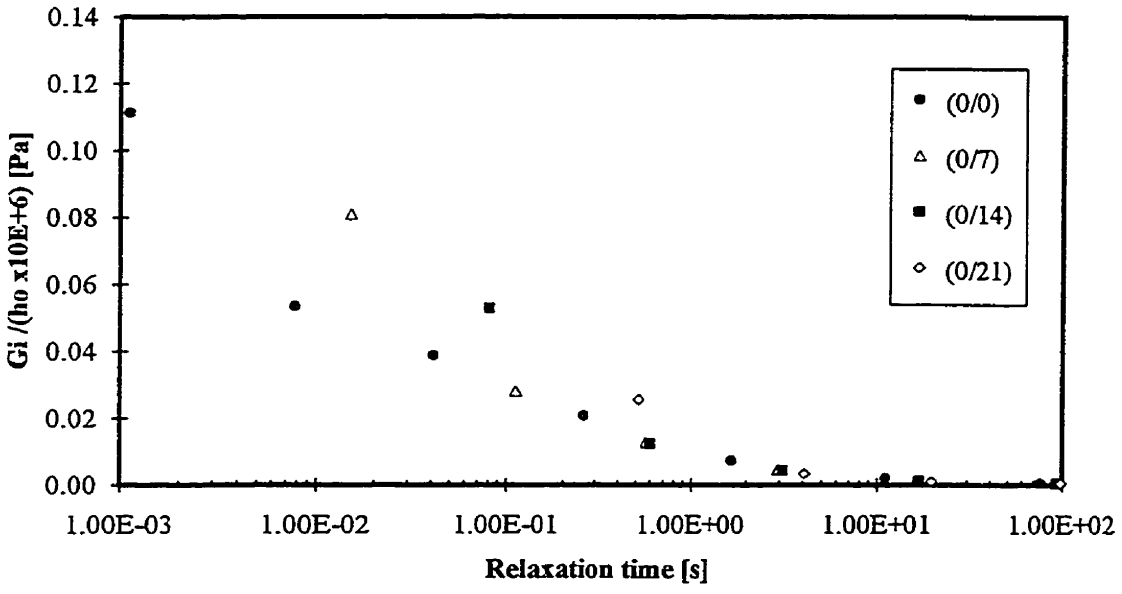

FIGURE 6.22 Impact of time-scale truncation at high frequency on the discrete spectrum of HDPE (IRIS).

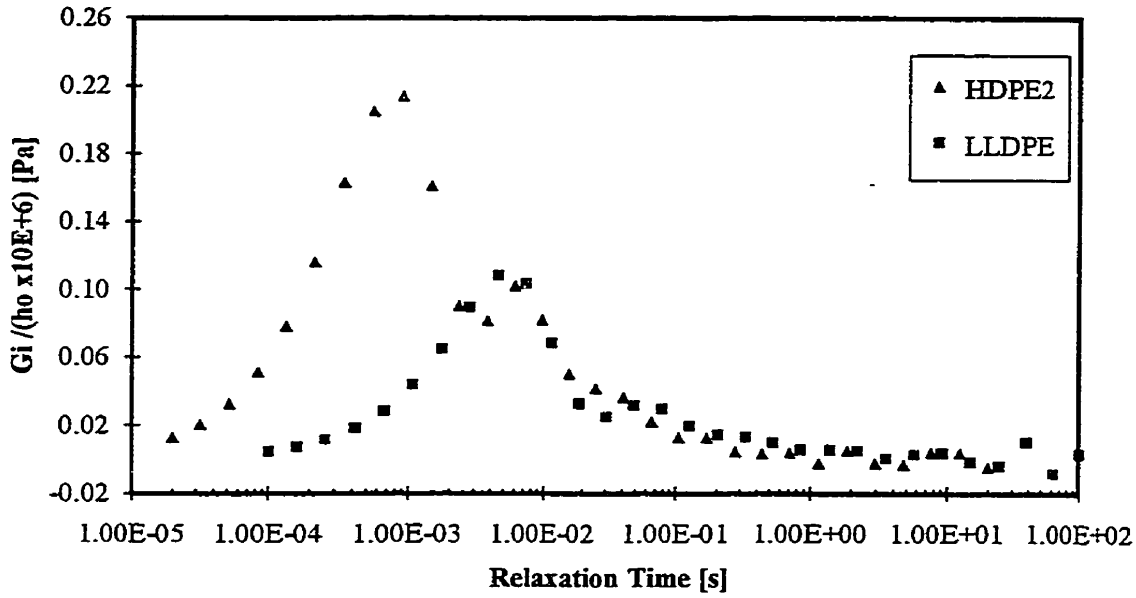

FIGURE 6.23 Relaxation spectrum of two other sets of polyethylene.

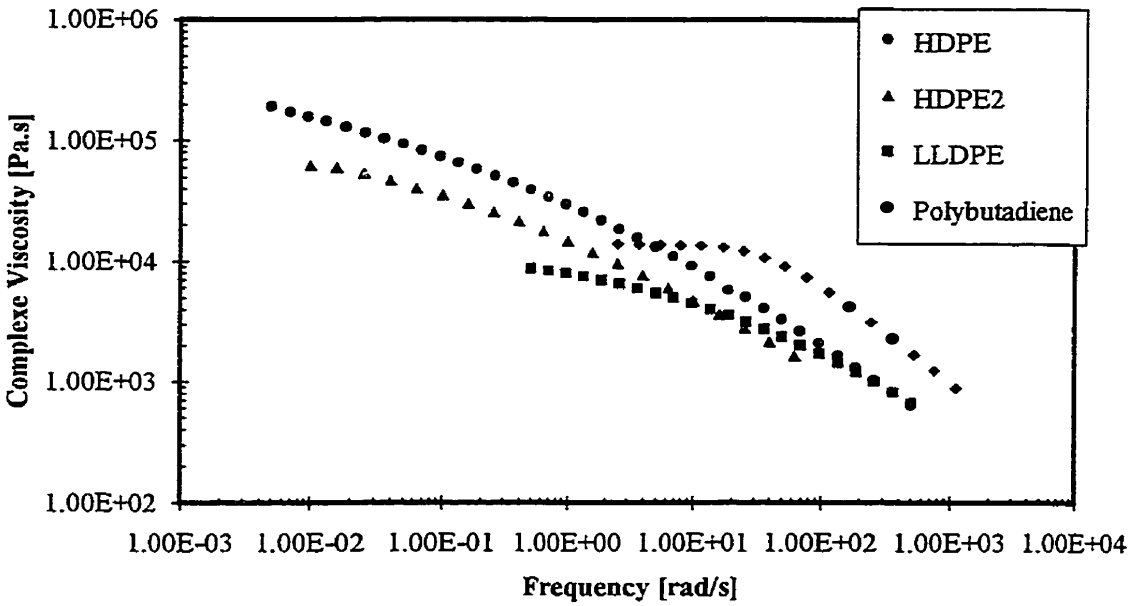

FIGURE 6.24 Comparison of the complex viscosity of the HDPE, HDPE2, LLDPE and polybutadiene samples.

6.3.3 Polybutadiene

LINEAR AND NONLINEAR REGRESSION

As in the case of HDPE, there is no "true" spectrum for the polybutadiene. We took the (0/0) spectrum as a reference since, according to the previous results, it is very close to the "true" spectrum. The data set was truncated at high frequency and at low frequency (1, and 2 decades were successively deleted). Truncation was also done at both ends. Each decade contains 6 points.

Figure 6.25 presents the relaxation spectra inferred using the linear regression (LR) for truncation at low frequency of the HDPE dynamic moduli. The spectra agree reasonably well with the (0/0) spectrum in the case of the linear regression. Of course, the higher the number of deleted decades, the further the inferred spectrum is from the reference spectrum (0/0). Similar results were obtained for the other truncations (high frequency and both ends) as well as in the case of the nonlinear regression method. As was noted before, the nonlinear regression method is usually more affected by truncation, and the deviation from the reference case is normally larger.

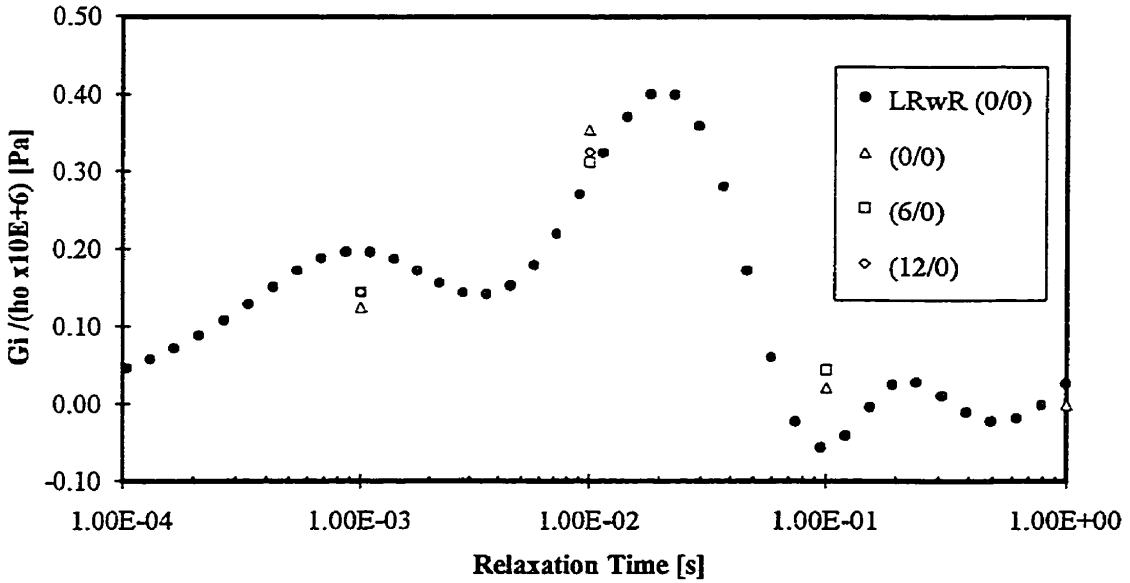

FIGURE 6.25 Impact of time-scale truncation at low frequency on the discrete spectrum of polybutadiene (LR).

Table 6.9 summarizes the behavior of the absolute average deviation between the recalculated moduli and the original moduli without truncation. Table E.8 and E.11 in Appendix E give the numerical values of the average deviation. As expected, the absolute deviation increases as the number of deleted decades increases for both methods.

TABLE 6.9 Summary of the impact of truncation on the absolute average deviation for recalculated dynamic moduli of polybutadiene (LR and IRIS).

Truncation	|AD| G' and |AD| G''
Truncation at high ω	|AD| ↗ as truncation ↗
Truncation at low ω	|AD| ↗ as truncation ↗
Truncation at both ends	Consistent

LINEAR REGRESSION with REGULARIZATION

It was possible to regularize the polybutadiene moduli, except when two decades of data were deleted at low frequency. By inspecting the complex viscosity curve of polybutadiene in Figure 6.23, we can see that this truncation corresponds to the plateau, and as soon as the plateau is missing, the regularization parameter becomes too small compared to the singular values, and several negative elastic moduli appear.

Figures 6.26 to 6.28 present the impact of truncation on the polybutadiene spectrum inferred with the regularization method (LRwR). The spectra are in good agreement. For truncation at high frequency, the first peak is missing in the spectrum. This peak corresponds to the information contained in the last decade of the moduli. Since the relaxation time range has been widened (Section 6.2), this peak disappears as soon as the first high frequency decade of data are deleted.

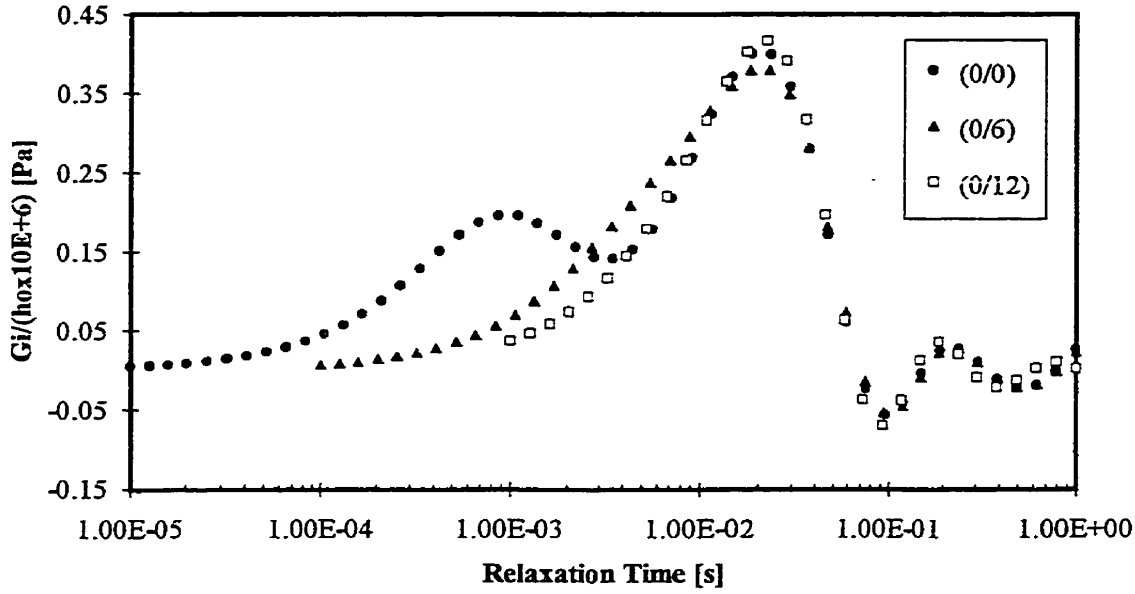

FIGURE 6.26 Impact of time-scale truncation at high frequency on the discrete spectrum of polybutadiene (LRwR).

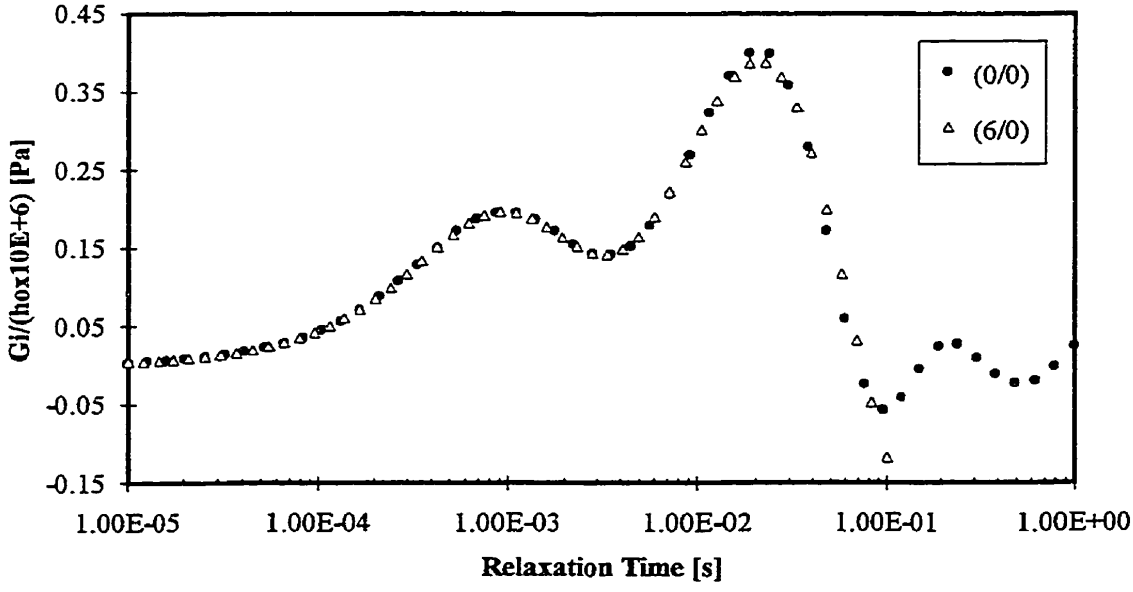

FIGURE 6.27 Impact of time-scale truncation at low frequency on the discrete spectrum of polybutadiene (LRwR).

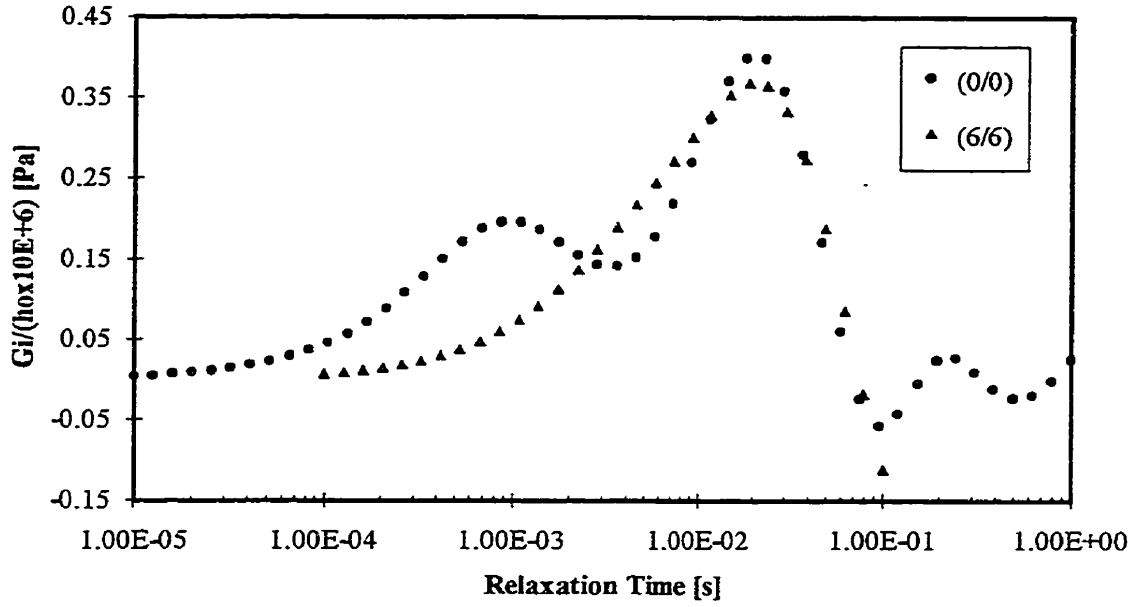

FIGURE 6.28 Impact of time-scale truncation at both ends on the discrete spectrum of polybutadiene (LRwR).

Table 6.10 summarizes the behavior of the absolute average deviation for the recalculated dynamic moduli using the spectra in Figures 6.26 to 6.28 (Table E.9 contains the numerical values of the average deviation and Table E.10 contains the regularization parameter). As expected, the average deviation increases as the number of data deleted increases.

TABLE 6.10 Summary of the impact of truncation on the absolute average deviation for recalculated dynamic moduli of polybutadiene (LRwR).

Truncation	|AD| G' and |AD| G''
Truncation at high ω	|AD| ↗ as truncation ↗
Truncation at low ω	|AD| ↗ as truncation ↗ Regularize only for (5/0)
Truncation at both ends	Consistent

The recalculated dynamic moduli were compared in all cases (linear regression with and without regularization and nonlinear regression) with the original moduli. The recalculated moduli were in very good agreement with the original moduli within the truncated range of frequency.

6.4. DATA ERRORS IMPACT ON THE SPECTRUM

The discrete spectra were calculated using the dynamic data presented in Section 5.3 for the HDPE. Only the nonlinear regression method (IRIS) was used to determine the discrete relaxation spectra since it gives better results than linear regression, and the regularization method cannot be used for the HDPE. This section presents the discrete relaxation spectrum for each set of dynamic modulus with data error. It is then possible to see the impact of gap size, edge shape, residual stress and temperature on the discrete linear spectrum.

Table 6.11 tabulates the average difference between dynamic moduli with data error and the reference dynamic moduli previously determined in Section 5.3. This table also describes the shape of the curves of modulus as a function of frequency (Figures 5.6b, 5.7b, 5.8b, 5.9b). The difference in the gap was 50 percent (1mm and 1.5mm) and the temperature difference was 30°C.

TABLE 6.11 Average difference between the dynamic moduli with data error and the reference dynamic moduli (values of Section 5.3).

Data Error	Diff. on G' (%)	Diff. on G'' (%)	Shape of the diff. curve
Gap size impact	27	27	Flat
Edge shape impact	22	24	Flat (increasing at beginning)
Residual stress impact	8	5	Decreasing
Temperature impact	21	14	Decreasing

Figures 6.29 and 6.30 show the impact of gape size and edge shape on the spectrum of HDPE. We see that in both of these cases the impact on the modulus is larger at short

relaxation times and gradually disappears at high frequency. The relaxation times are the same as for the reference case and the modulus is only shifted vertically to a lower value. The change in gap size results in the largest change in the G' and G'' curves (Table 6.11). Therefore, the change in gap size has the largest impact on the relaxation spectrum. Although the impact of gap size on the dynamic moduli (difference curve) was not a function of frequency, the impact on the spectrum decreased with increasing relaxation time.

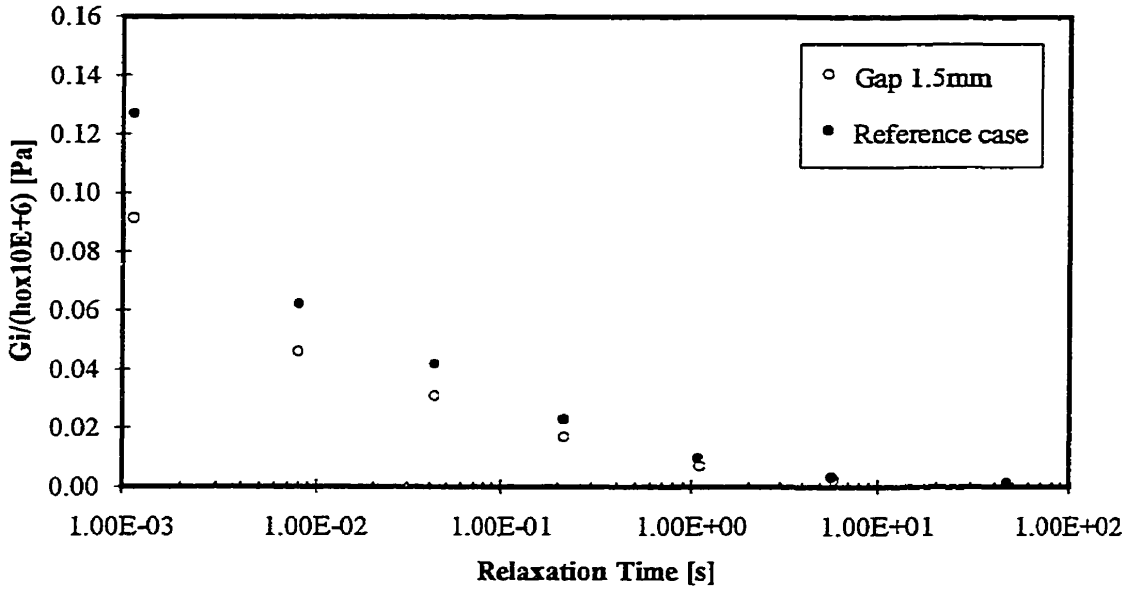

FIGURE 6.29 Impact of gap size on the discrete spectrum of HDPE (IRIS).

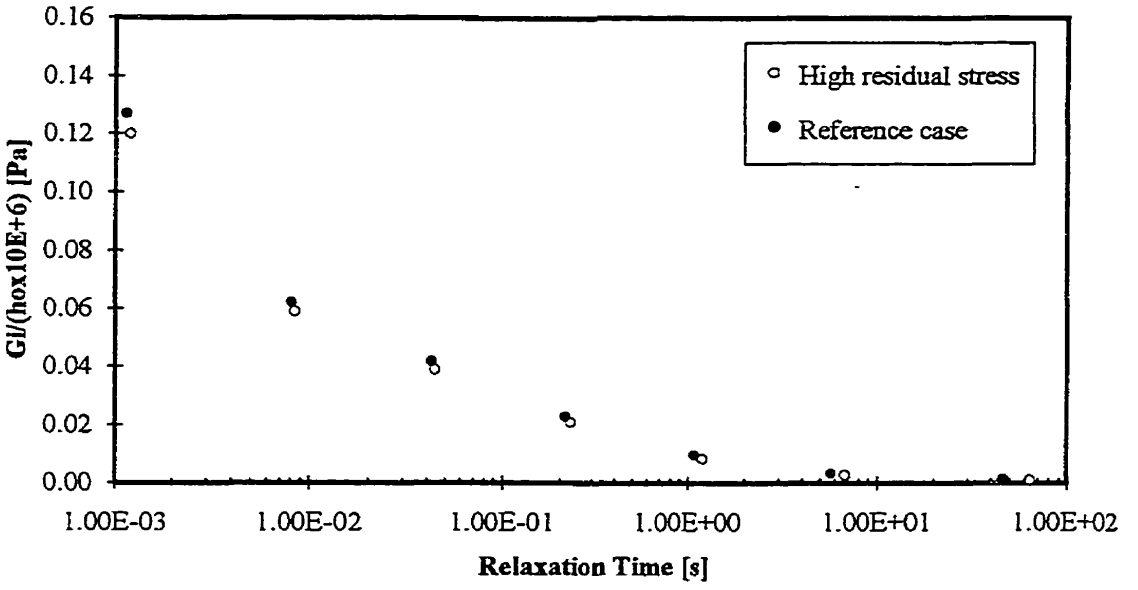

FIGURE 6.31 Impact of residual stresses on the discrete spectrum of HDPE (IRIS).

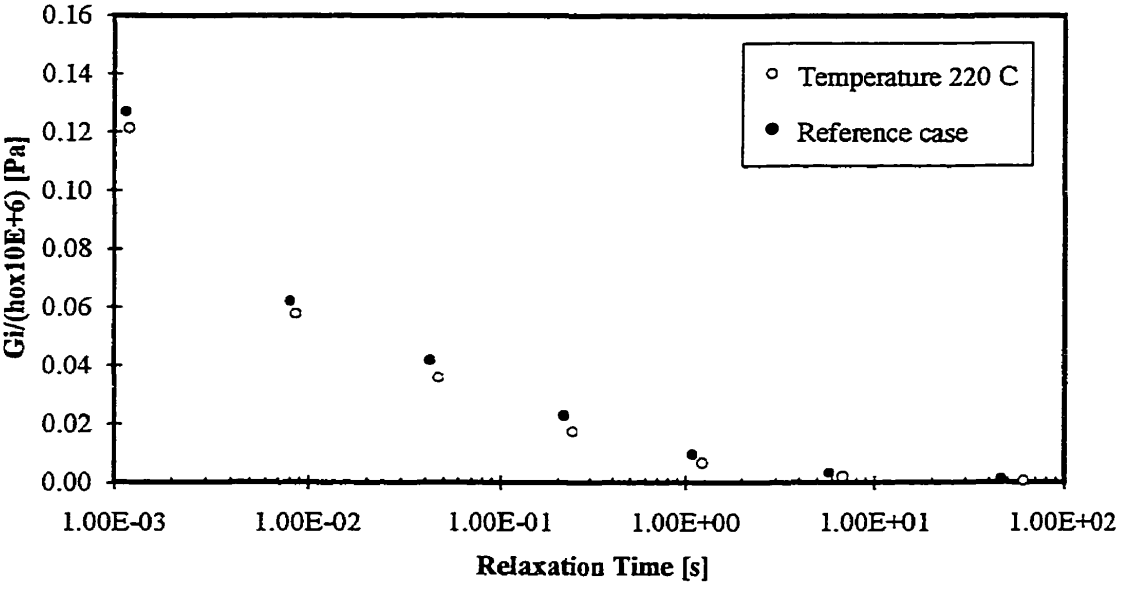

FIGURE 6.32 Impact of temperature on the discrete spectrum of HDPE (IRIS).

—CHAPTER 7—

7. CONCLUSIONS AND RECOMMENDATIONS

7.1 CONCLUSIONS

COMPARISON OF THE METHODS

The nonlinear regression and the regularization method give satisfactory results. The linear regression with regularization gives the smallest average deviation and permits one to obtain a reasonably detailed shape for the spectrum (high number of relaxation times). The nonlinear regression gives good results with a small number of relaxation times and is thus useful for use in a data bank. The linear regression gives the poorest results.

IMPACT OF POINT DENSITY

The impact of point density was found to be dependent on the method used to infer the spectrum and the dynamic modulus data (probably the number of available decades). In general, the impact is small, and it is possible to obtain good results with a density as low as two or three points per decade.

IMPACT OF TIME-SCALE TRUNCATION

Many data points can be left out without severely deforming the spectrum. This is especially true for linear regression with and without regularization. The spectrum inferred with truncated dynamic moduli is generally in good agreement with the one based upon the full moduli, if the relaxation times are within the corresponding frequency range. The worst results were obtained with the nonlinear regression. Each time the data set was truncated, the recalculated spectrum was in very good agreement with the original moduli, within the appropriate frequency range.

In all the cases except one, the average deviation increases as truncation increases. The regularization method and the nonlinear regression give the smallest deviation, although the nonlinear regression method was found to be the most susceptible to truncation. This perhaps means that although IRIS gives very good results from the mathematical point of view (obtaining of a recalculated spectrum as close as possible to the original one), it does not always reveal the true spectrum.

It is often difficult and time consuming to obtain experimental values at low frequencies or over a wide range of frequencies. It is then interesting to know the impact of time-scale truncation. According to the results found on the impact of time-scale truncation, we can say that the spectrum inferred within the relaxation times corresponding to the experimental frequency range is usually reliable.

It seems that the shape of the dynamic modulus curves has an impact on the ability of certain methods to infer the relaxation spectrum. This was the case for the regularization method applied to the HDPE and the simulated data. In those two cases, it seems important that the complex viscosity have a plateau at low frequency. The nonlinear regression was perhaps also affected by the shape of the spectrum in the case of the truncation at low frequency, since no clear trend was found. The reason is not the same as in the case of the regularization method, since the nonlinear method was able to handle the HDPE data. The particular shape of the simulated dynamic moduli curves probably contains important information for this method. This was impossible to verify since no mathematical information was available.

IMPACT OF DATA ERRORS

In the study of data errors, the impact on the dynamic moduli was reflected in the spectra. The vertical or horizontal shift found in the dynamic moduli was also found qualitatively in the spectra. We can conclude that calibration problems (vertical shift) or temperature problems(horizontal shift) in the dynamic moduli would be carried through into the spectra.

7.2 RECOMMENDATIONS

DETERMINATION OF THE SPECTRUM

A number of methods are available to infer the discrete and continuous relaxation spectra. Some of these are briefly presented at the end of Chapter 2. It would be interesting to do an exhaustive review and comparison of the methods currently available. Some of the methods proposed in the litterature incorporate a constraint that makes use of *a priori* knowledge about the solution rather than strictly numerical criteria (other than the fact that all the G_i should be positive). This could be quite useful in a study about time-scale truncation and data errors. There is still work to do concerning the "best" method to infer the relaxation spectrum.

TIME-SCALE TRUNCATION

It would be interesting to learn how data errors and truncation in the discrete spectrum influence the predictions of a nonlinear viscoelastic model based on the linear spectrum.

DATA ERRORS

In this work, the effect of data errors was studied in an experimental and empirical way only. It would be interesting to analyze the impact of data errors theoretically and quantitatively; to do a propagation of error analysis of the measurement process and its impact on the relaxation spectrum.

REFERENCES

1. Basistov, Yu. A., Yu. G. Yanovsky and D. A. Siginer, "A Minimax Method for the Determination of Relaxation Spectra," Proc. of 4th Eur. Rheol. Conf., 463-465 (1994).

2. Baumgaertel, M. and H. H. Winter, "Determination of the Discrete Relaxation and Retardation Time Spectra from Dynamic Mechanical Data," Rheol. Acta **28**, 511-519 (1989).

3. Baumgaertel, M. and H. H. Winter, "Determination of the Discrete Relaxation Time Spectrum from Dynamic Mechanical Data," ANTEC (1989).

4. Baumgeartel, M., A. Schausberger and H. H. Winter, "The Relaxation of Polymers with Linear Flexible Chains of Uniform Length," Rheol. Acta **29**, 400-408 (1990).

5. Baumgaertel, M. and H. H. Winter, "Interrelation Between Continuous and Discrete Relaxation Time Spectra," J. Non-Newt. Fluid Mech. **44**, 15-36 (1992).

6. Baumgaertel, M., *The Relaxation of Linear Flexible Polymers: Correlation Between Molar Mass Distribution and Rheological Data of Polymer Melts* (Ph.D. Thesis, University of Massachusetts, 1992).

7. Baumgaertel, M., M. E. De Rosa, J. Machado, M. Masse and H. H. Winter, "The Relaxation Time Spectrum of Nearly Monodisperse Polybutadiene Melts," Rheol. Acta **31**, 75-82 (1992).

8. Dealy, J. M. and K. F. Wissburn, *Melt Rheology and its Role in Plastics Processing* (Van Nostrand Reinhold, New York, 1990).

9. Elster, C. and J. Honerkamp, "The role of the Error Model in the Determination of the Relaxation Time Spectrum, " J. Rheol. **36**, 911-927 (1992).

10. Elster, C. and J. Honerkamp, "Modified Maximum Entropy Method and its Application to Creep Data," Macromolecules **24**, 310-314 (1991).

21. Kim, S. and S. J. Karrila, *Microhydrodynamics: Principles and Selected Applications* (Butterworth-Heinemann, Boston, 1991).

22. Mallows, C. L., " Some Comments on C_p," Technometrics **15**(4), 661-675 (1973).

23. Mead, D. W., "Numerical Interconversion of Linear Viscoelastic Material Functions," J. Rheol. **38**(6), 1769-1795 (1994).

24. Meissner, J., "Experimental Problems and Recents Results in Polymer Melt Rheometry," Makromol. Chem., Macromol. Symp. **56**, 25-42 (1992).

25. Orbey, N. and J. M. Dealy, "Determination of the Relaxation Spectrum from Oscillatory Shear data," J. Rheol. **35**(6), 1035-1049 (1991).

26. Press, W. H., B. P. Flannery, S. A. Teukolsky and W. T. Vetterling, *Numerical Recipies in Fortran; the Art of Scientific Computing* (Cambridge University, Cambridge, 1980).

27. Provencher, S. W., "A Constrained Regularization Method for Inverting Data Represented by Linear Algebraic or Integral Equations," Comput. Phys. Commun. **27**, 213-227 (1982).

28. Provencher, S. W., "CONTIN: a General Purpose Constrained Regularization Program for Inverting Noisy Linear Algebraic and Integral Equations," Comput. Phys. Commun. **27**, 229-242 (1982).

29. Simhambhatla, M. and A. I. Leonov, "The Extended Padé-Laplace Method for Efficient Discretization of Linear Viscoelastic Spectra," Rheol. Acta **32**, 589-600 (1993).

30. Soskey, P. R. and H. H. Winter, "Large Step Shear Strain Experiments with Parallel-Disk Rotational Rheometers," J. Rheol. **28**(5), 625-645 (1984).

31. Tchir, W. J. and P. C. Saucier, "Accuracy in Linear Viscoelastic Property Measurement: Effects of Instrument Compliance and Inertia Revisited," ANTEC (1994).

32. Tschoegl, N. W., *The Phenomenological Theory of Linear Viscoelastic Behavior* (Springer, New York, 1989).

33. Weese, J., "A Reliable and Fast Method for the Solution of Fredholm Integral Equations of the First Kind Based on Tikhonov Regularization," Comput. Phys. Commun. **69**, 99-111 (1992).

34. Weese, J., "A Regularization Method for Nonlinear Ill-Posed Problems," Comput. Phys. Commun. 77, 429-440 (1993).

35. Wiff, D. R. and M. Gehatia, "Inferring Mechanical Relaxation Spectra as an Ill-Posed Problem," J. Appl. Phys. **46**(10), 4231-4234 (1975).

36. Wiff, D. R., "RQP Method of Inferring a Mechanical Relaxation Spectrum," J. Rheol. **22**(6), 589-597 (1978).

37. Winter, H. H.,M. Baumgaertel and P. R. Soskey, "A Parsimonious Model for Viscoelastic Liquids and Solids," *Techniques in Rheological Measurement* (Chapman & Hall, London, 1993) Chap. 5.

APPENDIX A

LINEAR REGRESSION

```
% The purpose of that program is to determine N sets of (Gi,LAMBDAi) using M sets of data % [G',G"]. The N
values of LAMBDAi are equally distributed on a logarithmic time scale, % within the range of experimental
frequencies. The values of Gi are then determined by a % least-squares procedure, using a singular value
decomposition (SVD) method.
%
% The user enters the name of the file containing the spectrum [G', G"], the value of N   % (number of
lambdai wanted) and the coefficient of variation of the experimental [G', G"] % (TOL). The values of the
discrete spectrum [Gi, LAMBDAi] are saved in a file named      % RESUL.DAT. The program also recalculate the
values of the spectrum [G', G"] and stores % them in a file named GREC.DAT. The average absolute
deviations between the recalculated % spectrum [G', G"] and the original experimental spectrum [G', G"] are
also calculated.


pause
echo off
clc

clear


%---------%
% INPUT %
%---------%

% Load files
trunc=input('Enter a file name to convert (without extension):   ','s');
full=input('Enter the name of the file not truncated (without extension):   ','s');
trunspec=[trunc,'.dat'];
fullspec=[full,'.dat'];
eval(['load ', trunspec]);
eval(['load ', fullspec]);

% Create matrix WGG
wgg=eval([trunc]);
wggfull=eval([full]);

% M, N and tolerance (tol)
m=length(wgg);
mm=length(wggfull);
n=input('Enter the number of lambda wanted:   ');
tol=input('Enter the coefficient of variation of the experimental data:   ');

% lambdai minimum and maximum
```

```
    for k=2:n;
       g(k)=g(k-1)+((ub(2*m,k)*v(i,k))/(s(k,k)));
    end
    gg(i,1)=g(n)/equ;
end

% Display and save Gi
format short e
disp('Values of Gi:  ')
gg
save resul.dat lambda gg /ascii


%-----------------------------------------------%
%  Calculation of the number of negative Gi  %
%-----------------------------------------------%

% num
nu=find(gg<0);
num=length(nu);

disp('Number of negative Gi:  ')
num


%---------------------------%
%  Recalculate G' and G''  %
%---------------------------%

% G'
for i=1:mm;
   gp(1,1)=((gg(1,1)*equ*((wggfull(i,1)*lambda(1,1))^2))/(1+((wggfull(i,1)*lambda(1,1))^2)));
   for j=2:n;
      gp(j,1)=gp(j-1)+((gg(j,1)*equ*((wggfull(i,1)*lambda(j,1))^2))
                      /(1+((wggfull(i,1)*lambda(j,1))^2)));
   end
   g1(i,1)=gp(n,1);
end

% G''
for i=1:mm;
   gp(1,1)=((gg(1,1)*equ*(wggfull(i,1)*lambda(1,1)))/(1+((wggfull(i,1)*lambda(1,1))^2)));
   for j=2:n;
      gp(j,1)=gp(j-1,1)+((gg(j,1)*equ*(wggfull(i,1)*lambda(j,1)))
                      /(1+((wggfull(i,1)*lambda(j,1))^2)));
   end
   g2(i,1)=gp(n,1);
end

save grec.dat g1 g2 /ascii
```

```
%---------------------------------%
%  Difference between G and Grec  %
%---------------------------------%

% Difference
for i=1:mm;
   dif1(i,1)=abs(g1(i,1)-wggfull(i,2))/wggfull(i,2);
   dif2(i,1)=abs(g2(i,1)-wggfull(i,3))/wggfull(i,3);
end

% Average Absolute Deviation
avg(1,1)=mean(dif1);
avg(2,1)=mean(dif2);

disp('Average absolute deviation:   ')
avg


%-------------------------%
%  Standard error for Gi  %
%-------------------------%

for i=1:n;
   err(1)=((v(i,1))^2)/((s(1,1))^2);
   for j=2:n;
      err(j)=err(j-1)+(((v(i,j))^2)/((s(j,j))^2));
   end
   erro(i,1)=(sqrt((tol^2)*(err(n))))/gg(i,1);
end

disp('Error on Gi:   ')
erro
```

LINEAR REGRESSION WITH REGULARIZATION

```
% The purpose of that program is to determine N sets of (Gi, LAMBDAi) using M sets of data % [G', G"]. The
N values of LAMBDAi are equally distributed on a logarithmic time scale, % within the range of experimental
frequencies. The values of Gi are then determined by a % least-squares procedure, using a singular value
decomposition (SVD) method. To select  % the true solution from the set of possible solutions, an additional
criterion (the          % regularization parameter) is introduce by means of the Tikhonov Regularization
method.
%
% The user enter the name of the file containing the experimental data [w,G',G"], the     % value of N (number
of lambdai wanted), the coefficient of variation of the experimental
% G', G" (TOL) and the value of the regularization parameter (LAMBDA STAR). This last
% value must be previously calculated using the predictive mean-square signal error
% (subroutine LRwRmin).
%
% The values of the discrete spectrum [Gi, LAMBDAi] are saved in a file named RESUL.DAT.
% The program also recalculate the values of the spectrum G', G" and stores them in a
% file named GREC.DAT. The average absolute deviations between the recalculated spectrum
% G', G" and the original spectrum G', G" are also calculated.


pause
echo off
clc
clear


%----------%
%  INPUT  %
%----------%

% Load files
trunc=input('Enter a file name to convert (without extension):   ','s');
full=input('Enter the name of the file without truncation (without extension):   ','s');
trunspec=[trunc,'.dat'];
fullspec=[full,'.dat'];
eval(['load ', trunspec]);
eval(['load ', fullspec]);

% Create matrix WGG
wgg=eval([trunc]);
wggfull=eval([full]);

% M, N and tolerance (tol)
m=length(wgg);
mm=length(wggfull);
n=input('Enter the number of lambda wanted:   ');
tol=input('Enter the coefficient of variation of the experimental data:   ');

% lambdai minimum and maximum
```

```
lambda(1,1)=input('Enter lambdai minimum:    ');
lambda(n,1)=input('Enter lambdai maximum:    ');

% Lambda star
x=fmin('lrwrmin',0,3);


%-----------------------------------%
%  Create matrices LAMBDA and A  %
%-----------------------------------%

% LAMBDA
decade=log10(lambda(n,1))-log10(lambda(1,1));
for i=2:(n-1);
   lambda(i,1)=lambda(1,1)*10^((i-1)*(decade/(n-1)));
end

% A
for j=1:m;
   for i=1:n;
      a(j,i)=(((wgg(j,1)*lambda(i,1))^2)/(wgg(j,2)*(1+(wgg(j,1)*lambda(i,1))^2)));
   end
end
for j=1:m;
   k=j+m;
   for i=1:n;
      a(k,i)=((wgg(j,1)*lambda(i,1))/(wgg(j,3)*(1+(wgg(j,1)*lambda(i,1))^2)));
   end
end


%--------------%
%  SVD method  %
%--------------%

% 2m>n (condition necessary to apply SVD method)
if 2*m<n;
    for i=(2*m)+1:n;
       for j=1:n;
          a(i,j)=0;
       end
    end
    m=n/2;
end

% SVD method
[u,s,v]=svd(a,0);

% UB
for i=1:n;
   ub(1,i)=u(1,i);
   for j=2:(2*m);
```

```
      ub(j,i)=ub(j-1,i)+u(j,i);
   end
end

%----------------------%
%  Calculation of Gi  %
%----------------------%

% Constant to normalize Gi
equ=log(lambda(n,1)/lambda(1,1))/(n-1)

% Gi
for i=1:n;
   g(1)=((ub(2*m,1)*v(i,1))*(s(1,1)/(((s(1,1))^2)+x)));
   for k=2:n;
      g(k)=g(k-1)+((ub(2*m,k)*v(i,k))*(s(k,k)/(((s(k,k))^2)+x)));
   end
   gg(i,1)=g(n)/equ;
end

% Display and save Gi
format short e
disp('Values of Gi:  ')
gg
save resul.dat lambda gg /ascii


%-----------------------------------------------%
%  Calculation of the number of negative Gi  %
%-----------------------------------------------%

% num
nu=find(gg<0);
num=length(nu);

disp('Number of negative Gi:  ')
num


%---------------------------%
%  Recalculate G' and G''  %
%---------------------------%

% G'
for i=1:mm;
   gp(1,1)=((gg(1,1)*equ*((wggfull(i,1)*lambda(1,1))^2))/(1+((wggfull(i,1)*lambda(1,1))^2)));
   for j=2:n;
      gp(j,1)=gp(j-1,1)+((gg(j,1)*equ*((wggfull(i,1)*lambda(j,1))^2))
                        /(1+((wggfull(i,1)*lambda(j,1))^2)));
   end
   g1(i,1)=gp(n,1);
end
```

```
% G''
for i=1:mm;
   gp(1,1)=((gg(1,1)*equ*(wggfull(i,1)*lambda(1,1)))/(1+((wggfull(i,1)*lambda(1,1))~2)));
   for j=2:n;
      gp(j,1)=gp(j-1,1)+((gg(j,1)*equ*(wggfull(i,1)*lambda(j,1)))
                  /(1+((wggfull(i,1)*lambda(j,1))~2)));
   end
   g2(i,1)=gp(n,1);
end

save grec.dat g1 g2 /ascii


%-----------------------------------%
%  Difference between G and Grec  %
%-----------------------------------%

% Difference
for i=1:mm;
   dif1(i,1)=abs(g1(i,1)-wggfull(i,2))/wggfull(i,2);
   dif2(i,1)=abs(g2(i,1)-wggfull(i,3))/wggfull(i,3);
end

% Average Absolute Deviation
avg(1,1)=mean(dif1);
avg(2,1)=mean(dif2);

disp('Average Absolute deviation:  ')
avg




%                PREDICTIVE MEAN-SQUARE SIGNAL ERROR METHOD
%
%
% This subroutine determines the value of LAMBDA STAR using a predictive mean-square
% signal error method.  This subroutine is used with the main program LRwR.
%
% The user must previously enter the name of the file containing the experimental data
% [w ,G' ,G''], the value of N (number of lambdai wanted) and the coefficient of variation
% of the experimental data G', G'' (TOL) before calling LRwR.
%
%
function y=irwrmin(x)


%---------%
%  INPUT  %
%---------%
```

```
% Name of the data file containing the experimental data
% Coefficient of variation
% Number of lambdai
% Lambdai minimum
% Lambdai maximum

%%%%%%%%%%%%%%%%%%%%%%%%%
load simul.dat
wgg=simul;
tol=0.04;
n=30;
lambda(1,1)=0.001;
lambda(n,1)=100;
%%%%%%%%%%%%%%%%%%%%%%%%%

m=length(wgg);


%-----------------------------------%
%  Create matrices LAMBDA and A  %
%-----------------------------------%

% LAMBDA
decade=log10(lambda(n,1))-log10(lambda(1,1));
for i=2:(n-1);
   lambda(i,1)=lambda(1,1)*10^((i-1)*(decade/(n-1)));
end

% A
for j=1:m;
   for i=1:n;
      a(j,i)=(((wgg(j,1)*lambda(i,1))^2)/(wgg(j,2)*(1+(wgg(j,1)*lambda(i,1))^2)));
   end
end
for j=1:m;
   k=j+m;
   for i=1:n;
      a(k,i)=((wgg(j,1)*lambda(i,1))/(wgg(j,3)*(1+(wgg(j,1)*lambda(i,1))^2)));
   end
end


%-----------%
%SVD method %
%-----------%

% 2m>n (condition necessary to apply SVD method)
if 2*m<n;
    for i=(2*m)+1:n;
       for j=1:n;
          a(i,j)=0;
```

```
        end
    end
    m=n/2;
end

% SVD method
[u,s,v]=svd(a,0);

%UB
for i=1:n;
   ub(1,i)=u(1,i);
   for j=2:(2*m);
      ub(j,i)=ub(j-1,i)+u(j,i);
   end
end


%--------------------------------%
%  Calculation of LAMBDA star  %
%--------------------------------%

f1(1)=((x^2)/(((s(1,1)^2)+x)^2)*(ub(2*m,1)^2));
for i=2:n;
   f1(i)=f1(i-1)+((x^2)/(((s(i,i)^2)+x)^2))*(ub(2*m,i)^2);
end

f2(1)=((s(1,1)^2)/((s(1,1)^2)+x));
for i=2:n;
   f2(i)=f2(i-1)+((s(i,i)^2)/((s(i,i)^2)+x));
end

y=f1(n)+(2*(tol^2)*f2(n));
```

APPENDIX B

TABLE B.1 Simulated storage modulus (G'), loss modulus (G'') and complex viscosity (η^*) of the hypothetical material.

ω [rad/s]	G' [Pa]	G'' [Pa]	η^* [Pa.s]
1.00E-03	7.98E-05	4.12E-03	4.121773
1.61E-03	1.99E-04	6.96E-03	4.327231
2.59E-03	5.17E-04	9.69E-03	3.741529
4.18E-03	1.29E-03	1.79E-02	4.308135
6.72E-03	3.39E-03	2.43E-02	3.642074
1.08E-02	8.09E-03	3.80E-02	3.585504
1.74E-02	1.64E-02	6.22E-02	3.689702
2.81E-02	3.59E-02	8.59E-02	3.315969
4.52E-02	6.48E-02	1.18E-01	2.976101
7.28E-02	1.13E-01	1.45E-01	2.532372
1.17E-01	1.73E-01	1.80E-01	2.133781
1.89E-01	2.47E-01	1.90E-01	1.649322
3.04E-01	3.16E-01	1.97E-01	1.225119
4.89E-01	3.78E-01	1.67E-01	0.844582
7.88E-01	4.10E-01	1.52E-01	0.554614
1.27E+00	4.88E-01	1.40E-01	0.400056
2.04E+00	5.13E-01	1.37E-01	0.259952
3.29E+00	5.10E-01	1.47E-01	0.161368
5.30E+00	5.67E-01	1.60E-01	0.111279
8.53E+00	6.60E-01	1.67E-01	0.079791
1.37E+01	7.18E-01	2.09E-01	0.054433
2.21E+01	7.07E-01	1.82E-01	0.033026
3.56E+01	8.24E-01	1.93E-01	0.023759
5.74E+01	9.20E-01	1.45E-01	0.01623
9.24E+01	8.54E-01	1.23E-01	0.009339
1.49E+02	9.17E-01	9.10E-02	0.006196
2.40E+02	9.74E-01	5.32E-02	0.004072
3.86E+02	9.57E-01	4.03E-02	0.002482
6.21E+02	1.00E+00	2.50E-02	0.001611
1.00E+03	9.79E-01	1.73E-02	0.000979

TABLE B.2 Experimental storage modulus (G'), loss modulus (G'') and complex viscosity (η^*) of a narrow distributed polybutadiene.

ω [rad/s]	G' [Pa]	G'' [Pa]	η^* [Pa]
2.49E+00	2.05E+03	3.45E+04	13873.62
3.67E+00	4.16E+03	5.04E+04	13791.80
5.37E+00	8.85E+03	7.33E+04	13740.18
7.86E+00	1.88E+04	1.05E+05	13606.26
1.14E+01	3.77E+04	1.50E+05	13494.74
1.70E+01	7.47E+04	2.07E+05	12980.30
2.45E+01	1.36E+05	2.66E+05	12201.70
3.61E+01	2.24E+05	3.13E+05	10671.05
5.22E+01	3.25E+05	3.45E+05	9087.07
7.68E+01	4.32E+05	3.60E+05	7322.76
1.14E+02	5.35E+05	3.43E+05	5554.63
1.65E+02	6.19E+05	3.28E+05	4235.47
2.43E+02	7.01E+05	3.07E+05	3147.32
3.54E+02	7.73E+05	2.90E+05	2332.18
5.24E+02	8.42E+05	2.78E+05	1692.79
7.53E+02	8.97E+05	2.64E+05	1242.38
1.11E+03	9.56E+05	2.49E+05	887.06

APPENDIX C

SAMPLE PREPARATION METHOD NO.1

(Slow process - low residual stresses)

a) Heat the hydraulic press to 190°C (wait for constant temperature)
b) Place the mold filled with polymer pellets between the plates of the press
c) Heat 10 minutes (or until the temperature reaches 190°C)
d) Press slowly up to 10 000 pounds of pressure
e) Wait 10 minutes (keep pressure constant)
f) Press slowly up to 20 000 pounds of pressure
g) Wait 10 minutes (keep pressure constant)
h) Cool down (keep pressure constant)

SAMPLE PREPARATION METHOD NO.2

(Fast process - high residual stresses)

a) Heat the hydraulic press to 190°C (wait for constant temperature)
b) Place the mold filled with polymer pellets between the plates of the press
c) Heat 10 minutes (or until the temperature reaches 190°C)
d) Press quickly up to 20 000 pounds of pressure
e) Cool down immediately (keep pressure constant)

APPENDIX D

TABLE D.1 Dynamic moduli for the HDPE.

ω [rad/s]	G' [Pa]	G'' [Pa]	η^* [Pa.s]
5.00E-03	4.74E+02	8.31E+02	1.91E+05
6.95E-03	6.30E+02	1.05E+03	1.77E+05
9.65E-03	8.00E+02	1.34E+03	1.61E+05
1.34E-02	1.02E+03	1.67E+03	1.46E+05
1.86E-02	1.27E+03	2.09E+03	1.31E+05
2.59E-02	1.59E+03	2.59E+03	1.17E+05
3.60E-02	1.99E+03	3.22E+03	1.05E+05
5.00E-02	2.50E+03	3.98E+03	9.40E+04
6.95E-02	3.14E+03	4.90E+03	8.38E+04
9.65E-02	3.95E+03	6.01E+03	7.45E+04
1.34E-01	4.96E+03	7.35E+03	6.61E+04
1.86E-01	6.22E+03	8.93E+03	5.84E+04
2.59E-01	7.80E+03	1.08E+04	5.15E+04
3.60E-01	9.76E+03	1.30E+04	4.52E+04
5.00E-01	1.22E+04	1.56E+04	3.95E+04
6.95E-01	1.51E+04	1.85E+04	3.44E+04
9.65E-01	1.87E+04	2.18E+04	2.98E+04
1.34E+00	2.30E+04	2.55E+04	2.56E+04
1.86E+00	2.82E+04	2.96E+04	2.19E+04
2.59E+00	3.42E+04	3.41E+04	1.86E+04
3.60E+00	4.14E+04	3.89E+04	1.58E+04
5.00E+00	4.96E+04	4.41E+04	1.33E+04
6.95E+00	5.89E+04	4.95E+04	1.11E+04
9.65E+00	6.96E+04	5.52E+04	9.20E+03
1.34E+01	8.14E+04	6.11E+04	7.59E+03
1.86E+01	9.47E+04	6.70E+04	6.23E+03
2.59E+01	1.09E+05	7.30E+04	5.08E+03
3.60E+01	1.25E+05	7.89E+04	4.11E+03
5.00E+01	1.42E+05	8.49E+04	3.32E+03
6.95E+01	1.61E+05	9.07E+04	2.66E+03
9.65E+01	1.81E+05	9.64E+04	2.12E+03
1.34E+02	2.01E+05	1.02E+05	1.68E+03
1.86E+02	2.23E+05	1.08E+05	1.33E+03
2.59E+02	2.46E+05	1.13E+05	1.05E+03
3.60E+02	2.70E+05	1.19E+05	8.19E+02
5.00E+02	2.94E+05	1.25E+05	6.39E+02

TABLE D.2 Experimental storage modulus (G'), loss modulus (G'') and complex viscosity (η^*) of LLDPE.

ω [rad/s]	G' [Pa]	G'' [Pa]	η^* [Pa]
5.00E-01	9.80E+02	4.27E+03	8759.153
6.95E-01	1.44E+03	5.62E+03	8346.498
9.65E-01	2.10E+03	7.35E+03	7924.996
1.34E+00	3.03E+03	9.55E+03	7474.252
1.86E+00	4.33E+03	1.23E+04	7011.109
2.59E+00	6.11E+03	1.57E+04	6507.89
3.60E+00	8.53E+03	1.99E+04	6012.355
5.00E+00	1.18E+04	2.49E+04	5516.404
6.95E+00	1.60E+04	3.10E+04	5016.047
9.65E+00	2.16E+04	3.80E+04	4528.98
1.34E+01	2.86E+04	4.61E+04	4049.427
1.86E+01	3.75E+04	5.55E+04	3600.403
2.59E+01	4.85E+04	6.59E+04	3159.754
3.60E+01	6.19E+04	7.74E+04	2752.373
5.00E+01	7.80E+04	8.98E+04	2378.604
6.95E+01	9.70E+04	1.03E+05	2035.308
9.65E+01	1.19E+05	1.17E+05	1728.976
1.34E+02	1.44E+05	1.31E+05	1455.772
1.86E+02	1.73E+05	1.46E+05	1215.657
2.59E+02	2.05E+05	1.60E+05	1002.66
3.60E+02	2.39E+05	1.74E+05	821.899
5.00E+02	2.76E+05	1.88E+05	667.909

TABLE D.3 Experimental storage modulus (G'), loss modulus (G'') and complex viscosity (η^*) of HDPE2.

ω [rad/s]	G' [Pa]	G'' [Pa]	η^* [Pa]
1.00E-02	2.55E+02	7.11E+02	75497.57
1.59E-02	3.41E+02	9.28E+02	62350.08
2.51E-02	5.87E+02	1.39E+03	59884.46
3.98E-02	9.03E+02	1.94E+03	53636.97
6.31E-02	1.27E+03	2.67E+03	46885.26
1.00E-01	1.79E+03	3.61E+03	40325.42
1.59E-01	2.70E+03	4.91E+03	35339.7
2.51E-01	3.91E+03	6.51E+03	30224.58
3.98E-01	5.58E+03	8.56E+03	25674.27
6.31E-01	7.82E+03	1.11E+04	21507.12
1.00E+00	1.08E+04	1.42E+04	17866.53
1.59E+00	1.47E+04	1.81E+04	14710.36
2.51E+00	1.97E+04	2.27E+04	11959.46
3.98E+00	2.61E+04	2.81E+04	9622.927
6.31E+00	3.41E+04	3.44E+04	7672.906
1.00E+01	4.39E+04	4.17E+04	6056.32
1.59E+01	5.60E+04	5.01E+04	4740.641
2.51E+01	7.05E+04	5.97E+04	3677.607
3.98E+01	8.79E+04	7.06E+04	2832.748
6.31E+01	1.09E+05	8.30E+04	2166.078
1.00E+02	1.33E+05	9.71E+04	1647.25

APPENDIX E

TABLE E.1 Values of the regularization parameter as a function of point density for the polybutadiene and the simulated data.

Dynamic Moduli	Points/decade	λ^*
Polybutadiene	6	0.916
	3	0.781
	2	0.518
Simulated data	5	2.166
	3	1.331
	2	0.876

TABLE E.2 Impact of truncation on the absolute average deviation for recalculated dynamic moduli of simulated data (LR).

Truncation	|AD| G'	|AD| G''
(0/0)	6.20	9.94
(0/5)	6.38	15.01
(0/10)	9.14	26.65
(0/15)	16.59	42.90
(0/20)	31.25	57.65
(5/0)	11.43	9.86
(10/0)	16.61	10.70
(15/0)	58.52	47.04
(20/0)	95.17	79.06
(5/5)	11.62	15.01
(10/10)	19.63	27.61
(10/5)	16.90	15.84
(5/10)	14.71	26.68
(10/15)	22.37	42.43

TABLE E.3 Impact of truncation on the absolute average deviation for recalculated dynamic moduli of simulated data (LRwR).

Truncation	|AD| G'	|AD| G''
(0/0)	3.01	4.12
(0/5)	2.99	4.71
(0/10)	6.14	25.65
(0/15)	15.92	44.66
(0/20)	--	--
(5/0)	7.03	4.02
(10/0)	--	--
(15/0)	--	--
(20/0)	--	--
(5/5)	7.33	4.54
(10/10)	--	--
(10/5)	--	--
(5/10)	12.10	25.91
(10/15)	--	--

TABLE E.4 Regularization parameter as a function of truncation for simulated data.

Truncation	λ^*
(0/0)	2.166
(0/5)	2.300
(0/10)	0.308
(0/15)	2.082
(0/20)	--
(5/0)	1.735
(10/0)	--
(15/0)	--
(20/0)	--
(5/5)	1.368
(10/10)	--
(10/5)	--
(5/10)	0.578
(10/15)	--

TABLE E.5 Impact of truncation on the absolute average deviation for recalculated dynamic moduli of simulated data (IRIS).		
Truncation	**|AD| *G'***	**|AD| *G''***
(0/0)	3.12	4.37
(0/5)	4.31	5.17
(0/10)	4.02	4.57
(0/15)	15.90	42.12
(0/20)	25.01	52.79
(5/0)	30.85	4.51
(10/0)	15.05	5.69
(15/0)	33.68	20.07
(20/0)	27.57	18.56
(5/5)	30.63	4.34
(10/10)	12.63	25.22
(10/5)	14.92	63.94
(5/10)	7.52	25.76
(10/15)	17.08	44.88

TABLE E.6 Impact of truncation on the absolute average deviation for recalculated dynamic moduli of HDPE (LR).		
Truncation	**|AD| *G'***	**|AD| *G''***
(0/0)	2.85	3.46
(0/7)	4.48	13.93
(0/14)	16.20	33.81
(0/21)	37.23	55.60
(7/0)	5.32	3.32
(14/0)	20.03	5.68
(21/0)	36.24	16.43
(7/7)	7.46	13.84
(14/14)	32.52	35.44
(14/7)	23.32	17.22

TABLE E.7 Impact of truncation on the absolute average deviation for recalculated dynamic moduli of HDPE (IRIS).

Truncation	|AD| G'	|AD| G''
(0/0)	1.48	1.19
(0/7)	2.76	10.07
(0/14)	9.60	23.94
(0/21)	23.45	40.89
(7/0)	7.41	2.65
(14/0)	24.20	8.49
(21/0)	46.28	26.92
(7/7)	8.90	9.30
(14/14)	34.25	32.88
(14/7)	27.80	18.92

TABLE E.8 Impact of truncation on the absolute average deviation for recalculated dynamic moduli of polybutadiene (LR).

Truncation	|AD| G'	|AD| G''
(0/0)	16.67	13.74
(0/6)	16.16	21.14
(0/12)	65.85	85.29
(6/0)	54.64	11.16
(12/0)	42.41	22.18
(6/6)	51.36	21.26

TABLE E.9 Impact of truncation on the absolute average deviation for recalculated dynamic moduli of polybutadiene (LRwR).		
Truncation	**|AD| *G'***	**|AD| *G''***
(0/0)	0.75	0.91
(0/6)	1.29	7.83
(0/12)	2.26	15.14
(6/0)	6.89	0.98
(12/0)	--	--
(6/6)	7.61	7.55

TABLE E.10 Regularization parameter as a function of truncation for polybutadiene.	
Truncation	**λ^***
(0/0)	0.916
(0/6)	0.984
(0/12)	0.415
(6/0)	1.113
(12/0)	--
(6/6)	0.878

TABLE E.11 Impact of truncation on the absolute average deviation for recalculated dynamic moduli of polybutadiene (IRIS).		
Truncation	**|AD| *G'***	**|AD| *G''***
(0/0)	1.18	1.23
(0/6)	3.32	16.03
(0/12)	8.59	28.31
(6/0)	1.54	1.02
(12/0)	11.71	3.38
(6/6)	1.78	9.34

IMAGE EVALUATION TEST TARGET (QA-3)

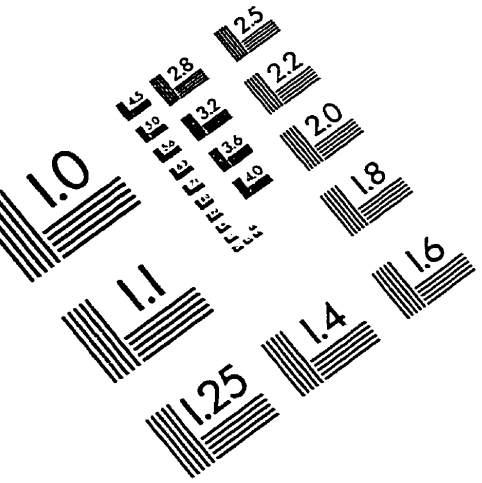

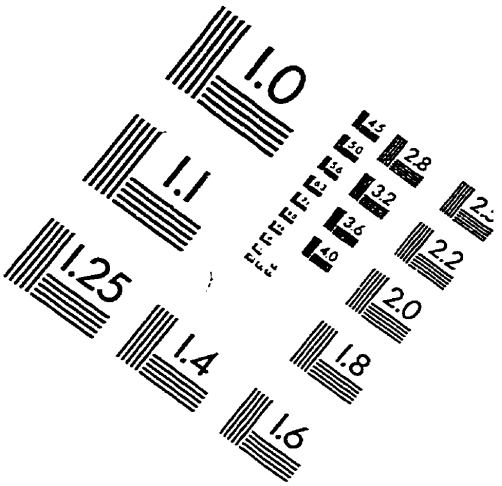

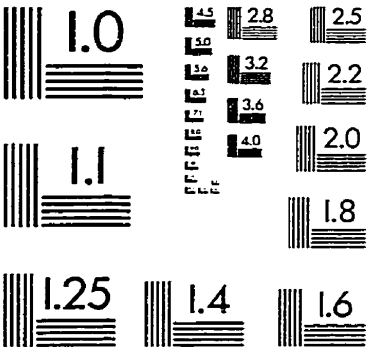

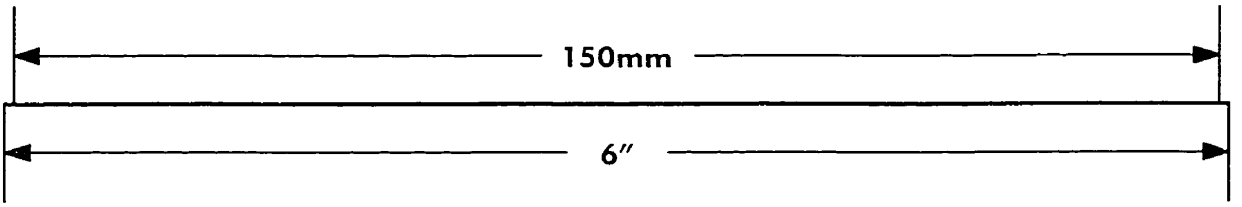

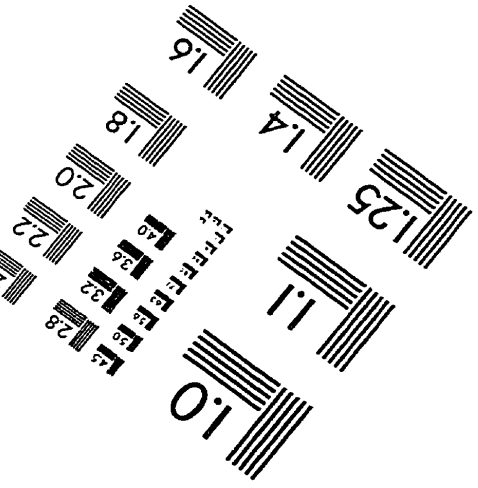

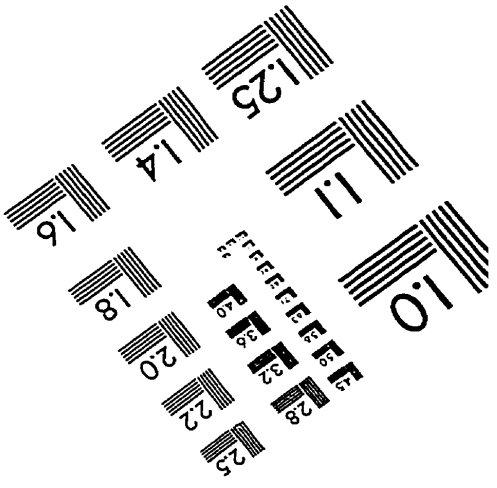

APPLIED IMAGE, Inc
1653 East Main Street
Rochester, NY 14609 USA
Phone: 716/482-0300
Fax: 716/288-5989